



00032481

Open file - Utah U

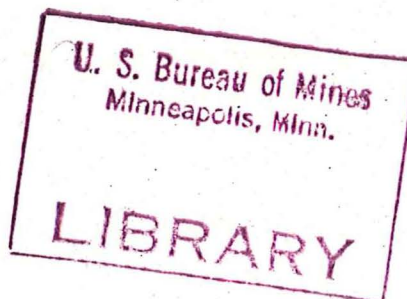
COPPER EXTRACTION FROM AMMONIA LEACH LIQUORS WITH HYDROXYOXIMES

Prepared for

UNITED STATES DEPARTMENT OF THE INTERIOR
BUREAU OF MINES

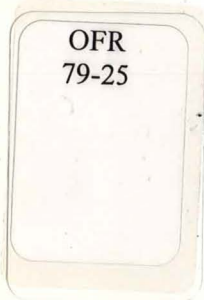
by

J.D. Miller
Professor of Metallurgy
University of Utah
Salt Lake City, Utah 84112



Final Report

Grant No. G0254033
Copper Extraction from Ammonia Leach Liquor with Hydroxyoximes



September, 1978

NOTICE

The views and conclusions contained in this document are those of the authors and should not be interpreted as necessarily representing the official policies or recommendations of the Interior Department's Bureau of Mines or of the U.S. Government.

FOREWORD

This report was prepared by the University of Utah, J.D. Miller, Department of Metallurgy, Salt Lake City, Utah 84112 under USBM Contract Number G0254033. The contract was initiated under the Bureau of Mines Metallurgy Program. It was administered under the technical direction of Mr. P.T. Brooks, Technical Project Officer. Mr. David J. Askin was the contract administrator for the Bureau of Mines.

This report is a summary of the work recently completed on this contract during the period June 30, 1975 to June 30, 1978, and submitted to USBM by the author in September, 1978.

TABLE OF CONTENTS

SUMMARY	7
INTRODUCTION	9
Chemistry of Copper Extraction	11
Kinetics of Copper Extraction	13
Heterogeneous Reactions	13
Kinetics of Copper Extraction in Acid Solution	14
Hydrodynamics of Liquid Spheres Moving in an Immiscible Liquid Field	16
Internal Mass Transfer for Liquid Spheres	19
External Mass Transfer to Liquid Spheres	21
Chemical Reaction at the Interface	23
Drop Size Distribution in a Mixer	24
EXPERIMENTAL	27
Materials	27
Stoichiometry of Extraction	27
Extraction Kinetics	28
Droplet Size Determination in a Mixer	30
Agitation Equipment	30
Range of Operation	31
Droplet Size Measurement	31
RESULTS AND DISCUSSION	34
Equilibrium Study	34
Effect of Free Ammonia	34
Effect of pH	37
Kinetic Study	40
Rising Drop Experiments	40
Effect of Reactant Concentration	41
Effect of Temperature	43
Comparison of Theory with Experimental Results	48
Kinetics of Extraction for Different Chelating Extractants	50
Change in Rate Control from Internal Mass Transfer to External Mass Transfer	50
Falling Drop Experiments	53
Effect of Reactant Concentration	53
Comparison of Theory with Experimental Results	60
Drop Size Distribution in a Mixer	64
CONCLUSIONS	68
REFERENCES	70

LIST OF FIGURES

Figure 1.	Schematic representation of the heterogeneous reaction involved in solvent extraction systems.	15
Figure 2.	Terminal velocity and internal flow pattern for a liquid sphere as a function of drop diameter.	17
Figure 3.	Representation of the relative importance of transport processes in the continuous and in the dispersed phase for various reactant concentration ratios. Intersection of horizontal dashed line with diagonal line indicates the critical time (t_c) during which the rate is limited by mass transfer in the continuous phase. Conditions: $D_c = 7.5 \times 10^{-6}$ cm ² /sec, $D_d = 4 \times 10^{-6}$ cm ² /sec, $a = 0.1$ cm. $\mu_c = 1$ cp $\mu_d = 1.68$ cp, $v = 10$ cm/sec, $v_d = 2$, $v_c = 1$ ($v =$ stoichiometric number).	22
Figure 4.	Classification of Impellers by their flow pattern.	25
Figure 5.	Schematic diagram of Single Drop Reaction Cell (SDRC).	29
Figure 6.	Schematic diagram of agitation vessel.	32
Figure 7.	IR spectra of organic phase obtained from both acidic and ammoniacal solutions.	35
Figure 8.	Effect of ammonia concentration on copper extraction at constant pH (10.2-10.5).	36
Figure 9.	Slope Analysis plot indicative of the number of ammonia molecules coordinated by the cupric ion under the conditions specified in Figure 8.	38
Figure 10.	Effect of pH on copper extraction at a constant total ammonia concentration of 0.5 M.	39
Figure 11.	Rate of copper extraction into rising drops for various dispersed (organic) and continuous (aqueous) phase concentrations.	42
Figure 12.	Parabolic plot of rate data illustrating that the kinetics conform to the linear relationship required for rate control by internal mass transfer.	44

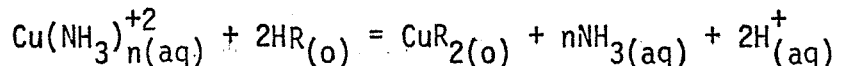
Figure 13.	Reaction order plot illustrating the first order dependence on the extractant concentration in the dispersed phase. Vertical bars indicates the range of the rate for all the copper concentration in the continuous phase. Note that the rate is independent of copper concentration in continuous phase.	45
Figure 14.	Parabolic plot of rate data for extraction into rising drops at various temperatures.	46
Figure 15.	Arrhenius plot of the rate data presented in Figure 14. . . .	47
Figure 16.	Comparison of experimental results with theoretical predictions for rate control by internal mass transfer (See equations 15 and 18) showing the concentration effect.	49
Figure 17.	Comparison of experimental results with theoretical mass transfer showing the drop size effect.	51
Figure 18.	Parabolic plot of rate data for different chelating extractants. Note that the kinetics are essentially independent of the extractant and that 'no' catalytic effect from LIX 63 is observed.	52
Figure 19.	Evaluation of the "A" parameter, $(Cu)_{c,o}/(LIX)_{d,o}$ which theoretically determines the point at which mass transfer resistance becomes predominant. For $A > 0.05$ reaction rates will be limited by internal mass transfer.	54
Figure 20.	Evaluation of parameter "A," $(Cu)_{c,o}/(LIX)_{d,o}$ which theoretically determines the point at which external mass transfer resistance becomes predominant. For $A < 0.05$ reaction rates will be limited by external mass transfer.	55
Figure 21.	Rate of copper extraction from falling drops for various initial copper concentrations.	56
Figure 22.	Rate of copper extraction from falling drops for various initial LIX 64N concentration.	57
Figure 23.	Parabolic plot of rate data for small drop size illustrating that the kinetics conform to the linear relationship required for rate control by internal mass transfer.	58
Figure 24.	Parabolic plot of rate data for large falling drops illustrating that the kinetics conform to the linear relationship required for rate control by internal mass transfer.	59

Figure 25.	Reaction order plot illustrating the first order dependence on the copper concentration in the dispersed phase.	61
Figure 26.	Comparison of experimental results with theoretical predictions for rate controlled by internal mass transfer for various copper concentrations (Eqs. 15 and 18). Data taken from Figures 22 and 23.	62
Figure 27.	Comparison of experimental results with theoretical prediction for rate controlled by internal mass transfer for various drop sizes.	63
Figure 28.	Combination effect of drop size and concentration on extraction kinetics compared with theoretical prediction for internal mass transfer. The kinetics of extraction in acidic solution is also shown which illustrate the rate is slower and not controlled by mass transfer process.	65
Figure 29.	A comparison of experimental drop size distribution data and those predicted by the simplified model equation: $f_0(v) = (1/v_0) \exp(-v/v_0)$. Experimental data by various investigators (References 31, 32, 33 and 34).	67

SUMMARY

During the past two years the USBM has sponsored a research program at the University of Utah to study the chemistry of copper extraction from ammoniacal solutions by hydroxyoxime extractants. Equilibrium measurements were made by shake-out experiments with subsequent analysis of the aqueous and/or organic phases. The kinetic experiments were carried out in a single drop reaction cell (SDRC) in order to establish the details of the intrinsic reaction kinetics for the system. Drop size distributions generated in a mixer were determined by an encapsulation technique followed by size analysis.

The equilibrium measurements indicate the extraction involves a complete displacement of ammonia ligands from the coordination sphere of the cupric ion by the extractant molecules. The extraction reaction has the following stoichiometry;



The extraction coefficient was found to be sensitive to the ammonia concentration and the pH of the system. These results were interpreted in terms of the mass action expression and explained by taking into consideration the stability of the various cupric ammine complexes,

$$\log D = \log k - \log \left(1 + \sum_{i=1}^6 \beta_i [\text{NH}_3]^i \right) + 2 \log [\text{HR}]_{(\text{o})} + 2\text{pH}$$

From single drop experiments, the kinetics of extraction appear to be controlled by mass transfer in the dispersed phase. The reaction has a low apparent activation energy of 2.6 kcal/mole. Based on first principles, the mass transfer process was explained to be due to molecular diffusion for small drop sizes which behaved as stagnant drops, while

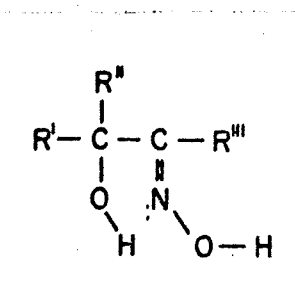
convective transport contributes significantly to the reaction rate for larger drop sizes due to internal circulation patterns which develop under certain circumstances. The results also indicate that the rate of copper extraction from ammonia solutions is considerably faster than from acidic solution. This was to be expected in as much as extraction from acidic solution has been reported to be controlled by a surface chemical reaction having an apparent activation energy from 7 to 15 kcal/mole.

The drop size distribution in an agitation vessel seems to follow an exponential distribution in terms of the number density function. The drop size increases as the phase fraction (volume of organic/total volume of both liquid phases) increases. Further research needs to be done in order to synthesize this information on intrinsic reaction kinetics and drop size distribution and establish a detailed explanation of the extraction kinetics observed for a mixer.

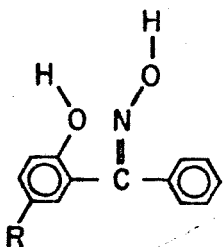
INTRODUCTION

A significant research effort has been devoted to develop ammonia oxidation leaching processes for copper sulfide concentrate^(1,2) and low grade native copper ore.⁽³⁾ This has lead to process development studies and finally to construction of plants to treat copper sulfide concentrates and copper scrap.⁽²⁾ When compared with conventional sulfuric acid leaching processes, the major advantage of ammoniacal systems is their ability to reject iron and many acid consuming gangue minerals.

An important unit operation in any hydrometallurgical process is the concentration and purification of the leach liquor for electrolysis, which frequently is accomplished by solvent extraction. A major extractant for the recovery of copper from ammoniacal solution has been the hydroxyoximes; chelating extractants such as the LIX reagents developed by General Mills. Currently other companies such as Shell Chemicals Ltd. and Acorga Ltd. produce similar extractants. The most widely used extractant, however, is LIX 64N a mixture of hydroxyoximes. This extractant consists of two components, the aliphatic α hydroxyoxime (LIX 63),



and the aromatic β hydroxyoxime (LIX 65N)



The β hydroxyoxime is capable of existing as either the syn- or anti-isomer. Only the anti-form which is capable of copper extraction is shown above.

A considerable amount of research has been done on the extraction of copper from acidic solutions both with regard to equilibrium and kinetic behavior. (4,5,6,7) Very little is known about important factors which determine the equilibrium and kinetic behavior of copper extraction from the ammoniacal solutions.

During the past two years a research program has been sponsored by the USBM at the University of Utah in which three major subjects related to copper extraction from ammoniacal solution by LIX 64N reagents have been investigated. These areas are: chemistry of extraction, kinetics of extraction and drop size measurements in a stirred tank reactor. The ultimate objective is to establish the fundamental chemistry, the intrinsic reaction kinetics and the mixing behavior in a stirred tank reactor in order to be able to eventually describe the rate of extraction in a mixer. As

a result of this research program, several papers have been prepared for presentation at professional society meetings:

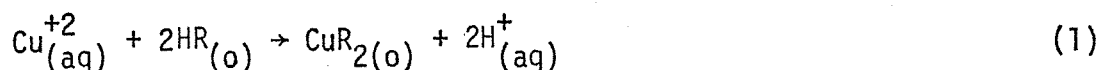
1. J.D. Miller, "Solvent Extraction Reaction Kinetics," presented in ACS Centennial Meeting at San Francisco, September 1976.

2. E.F.S. Pereira, H.H. Haung and J.D. Miller, "Mass Transfer in Solvent Extraction Single Drop Reaction System," presented at 16th Annual Conference of Metallurgists, CIMM, August 21, 1977 at Vancouver, Canada.

3. E.F.S. Pereira, H.H. Haung and J.D. Miller, "Copper Extraction from Ammoniacal Solutions by Chelating Extractants," presented at AIME Annual Meeting in Denver, March 1, 1978.

Chemistry of Copper Extraction

The chemistry of copper extraction from acidic solution by hydroxy-oxime reagents has been intensively investigated by several researchers.^(6,8) Spectrophotometric⁽⁴⁾ evidence indicates that a copper-LIX complex is the extraction product and stoichiometric study reveals the following chemical reaction;



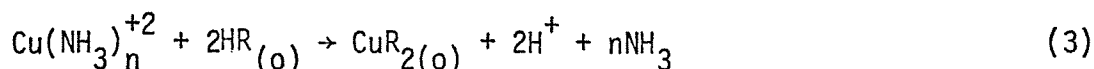
The extraction coefficient (copper concentration in the organic phase divided by copper concentration in aqueous solution) can be calculated from the equilibrium constant K;

$$\log D = \log K + 2 \log [\text{HR}]_{(\text{o})} + 2\text{pH} \quad (2)$$

where E = extraction coefficient = $[\text{CuR}_2]_{(\text{o})} / [\text{Cu}]_{\text{total}(\text{aq})}$
K = equilibrium constant including activity coefficients for Equation 1

$[\text{HR}]_{(o)}$ = concentration of extractant in organic phase.

In the ammoniacal system the cupric ion in the aqueous solution is no longer a predominant species but exists as cupric-amine complexes. The extraction of copper from these solutions could be represented in the following way;



Thermodynamically, however, the copper extraction equation written for acidic solutions, Equation 1, can still be applied to the ammonia system, but the activity of the cupric ion will be much lower than the total copper concentration. In ammoniacal solution, cupric ion concentration can be calculated from the overall stability constants of the cupric ammine complexes defined as,

$$\beta_i = \frac{[\text{Cu}(\text{NH}_3)_i^{+2}]_{(aq)}}{[\text{Cu}^{+2}]_{(aq)} [\text{NH}_3]_{\text{free}(aq)}^i} \quad (4)$$

where $[\text{Cu}(\text{NH}_3)_i^{+2}]_{(aq)}$ = concentration of the i th cupric ammine complex in aqueous solution,

$[\text{Cu}^{+2}]_{(aq)}$ = concentration of cupric ions in aqueous solution,

$[\text{NH}_3]_{\text{free}(aq)}$ = concentration of free ammonia in aqueous solution.

The overall stability constants, β_i values, for cupric-amine complexes are listed below,

$$\log \beta_1 = 4.15 \quad \log \beta_2 = 7.65 \quad \log \beta_3 = 10.54$$

$$\log \beta_4 = 12.67 \quad \log \beta_5 = 12.17 \quad \log \beta_6 = 9.67$$

If metal hydrolysis can be ignored, then the fraction of cupric ion to total copper concentration in the aqueous phase can be evaluated,

$$[\text{Cu}^{+2}]_{(\text{aq})} / [\text{Cu}]_{\text{total}(\text{aq})} = 1 / (1 + \sum_{i=1}^6 \beta_i [\text{NH}_3]_{\text{free}(\text{aq})}^i) \quad (5)$$

As a result, an additional term will be contributed to the expression for the copper extraction coefficient,

$$\log E = \log K - \log (1 + \sum_{i=1}^6 \beta_i [\text{NH}_3]_{\text{free}(\text{aq})}^i) + 2 \log [\text{HR}]_{(\text{o})} + 2\text{pH} \quad (6)$$

This equation indicates that the pH has a positive effect and that the ammonia concentration has a negative effect on copper extraction. From examination of the stability constants for the cupric-ammine complexes, it is seen that the tetra-ammine copper (II) ion and the penta-ammine copper (II) ion have the highest β_i values. This suggests that in normal ammoniacal leaching systems, concentration of free ammonia about 16 g/l, the average number of ammine ligands coordinated to a cupric ion will be between 4 and 5.

Kinetics of Copper Extraction

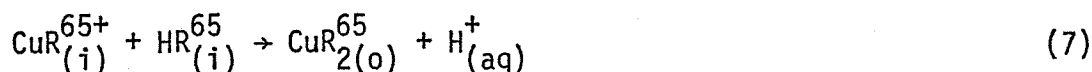
Heterogeneous Reactions

Solvent extraction involves the reaction between two immiscible liquids, one liquid can be considered the dispersed phase consisting of drops suspended in the other liquid which would be the continuous phase. Due to the low solubility of the reactants in the opposite phase ($\text{Cu}(\text{NH}_3)_n^{++}$ in the organic and the hydroxyoxime in the aqueous), the reaction will usually take place at the liquid/liquid interface. For the reaction to proceed, the reactants in the dispersed phase have to be transported to

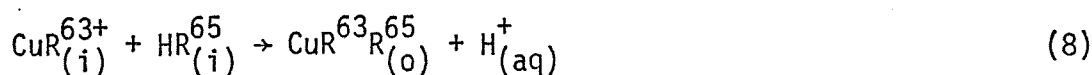
the interface by internal mass transfer, the reactants in the continuous phase have to be transported to the interface by external mass transfer, and finally chemical reaction occurs at the interface. See Figure 1. The rate of extraction usually will be limited by the slowest of these steps.

Kinetics of Copper Extraction in Acidic Solution

Recently, several fundamental kinetic studies have been reported on the extraction of copper by LIX reagents in acidic systems.^(7,8) These studies have employed a variety of experimental techniques. The results indicate that the rate of copper extraction by LIX 65N/LIX 63 reagents is controlled by chemical reaction at the aqueous/organic interface. Results from experiments with the AKUFVE system by Flett⁽⁸⁾ and the Lewis cell by Fleming⁽⁹⁾ indicate that the rate limiting step is the addition of the second ligand at the interface. That is, for LIX 65N only,



or for LIX 65N and LIX 63,



The rate of reaction can be expressed as,

$$-\frac{d(\text{Cu}^{+2})}{dt} = k[\text{Cu}^{+2}]_{(aq)} [\text{LIX 65N}]_{(o)} [\text{LIX 63}]_{(o)}^{1-0.5} [\text{H}^{+}]_{(aq)}^{-1} \quad (9)$$

where $[\text{LIX 65N}]_{(o)}$, $[\text{LIX 63}]_{(o)}$ = concentrations of LIX 65N and LIX 63, respectively in organic phase.

The single drop technique by Atwood⁽⁷⁾ has indicated that the rate of extraction is independent of hydrogen ion concentration at relatively high pH values (2.21-4.98) and the rate expression obtained was,

HETEROGENEOUS REACTION
IN SOLVENT EXTRACTION
PHASE 2

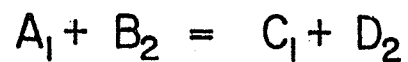
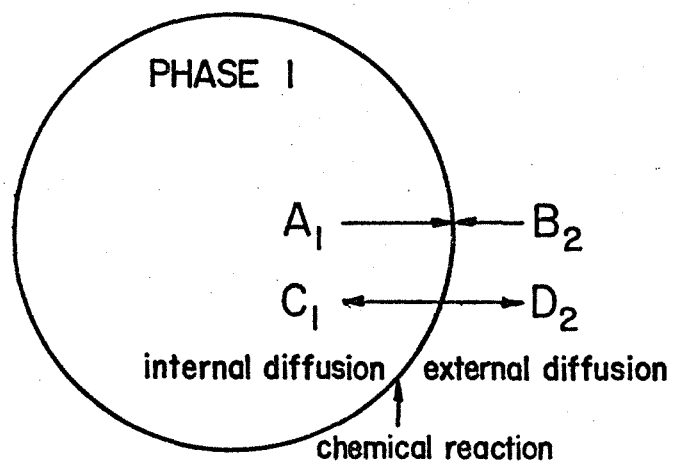


Figure 1. Schematic representation of the heterogeneous reaction involved in solvent extraction systems.

that the rate curves for all temperatures are parabolic which indicates that the rate controlling step does not change in the temperature range studied. In this case the parabolic plot has been normalized with respect to the initial concentration of the extractant in the dispersed phase, so that equation 24 is rearranged in the following form.

$$\frac{\Delta[\text{HR}]_{d,t}}{[\text{HR}]_{d,0}} = k \cdot D^{1/2} \sqrt{t/a^2} \quad (26)$$

Note that the slope of this plot is equal to $k \cdot D^{1/2}$. The Arrhenius plot in Figure 15 reveals a low apparent activation energy of 2.6 kcal/mole.

Comparison of theory with experimental results. In order to theoretically predict the internal mass transfer for both the stagnant model (Equation 13) and the circulation model (Equation 16), the diffusion coefficient of LIX 64N in Escaid 200 has to be known and was estimated by the Wilke and Chang method⁽²⁷⁾ to be $4.34 \times 10^{-6} \text{ cm}^2/\text{sec}$. A close agreement between experimental data and theoretical predictions is seen in Figure 16. Figure 16 shows the comparison for several concentrations of LIX 64N for both small and large drop sizes. The results indicate that the rate follows the stagnant model (molecular diffusion), equation 15, for the LIX 64N concentrations greater than 5%, and that the rate follows the circulation model (convective transport plus molecular diffusion), equation 18, for LIX 64N concentrations less than 5%. This analysis which indicates a change from the circulation model to the stagnant model for an increase in LIX concentration is reasonable because both the viscosity of the organic solution and the organic/aqueous interfacial tension increase as the LIX 64N concentration increases.^(28,29) As a result, the drop tends to circulate

$$-\frac{d(\text{Cu}^{+2})}{dt} = k[\text{Cu}^{+2}]_{(\text{aq})}[\text{LIX } 65\text{N}]_{(\text{o})}^{0.5}[\text{LIX } 63]_{(\text{o})}^{0.5} \quad (10)$$

The rate controlling step was suggested to be addition of the first extractant molecule



Hydrodynamics of Liquid Spheres Moving Through an Immiscible Liquid Field

Among the three techniques that have been used for the study of extraction kinetics; the AKUFVE system, the Lewis cell and the Single Drop Reaction Cell (SDRC), the single drop technique seems to have two unique features; the determined interfacial area and the better defined hydrodynamic behavior of liquid spheres.

Liquid spheres differ from solid spheres in that the dispersed liquid can be set in motion by the viscous drag from the continuous liquid through which the drop moves. Additionally, drops can be subjected to deformation because of the differences in pressure acting on various parts of the surface. As a result of these considerations, the terminal velocity of a liquid drop may have a significant difference from the corresponding velocity for a solid sphere. Figure 2 shows the terminal velocity of a liquid drop as a function of the drop diameter. Three distinct regions can be identified.^(10,11,12) For small drops in region A, the liquid boundary layer inside the drop remains rigid and the liquid drop will be spherical in shape and behave like a solid sphere. The terminal velocity will generally be that of a solid sphere of equal size and density moving in the same continuous phase. In region B, the boundary layer inside the drop will no longer remain rigid, and the momentum from the continuous phase will be transferred to the drop which develops internal circulation. Under

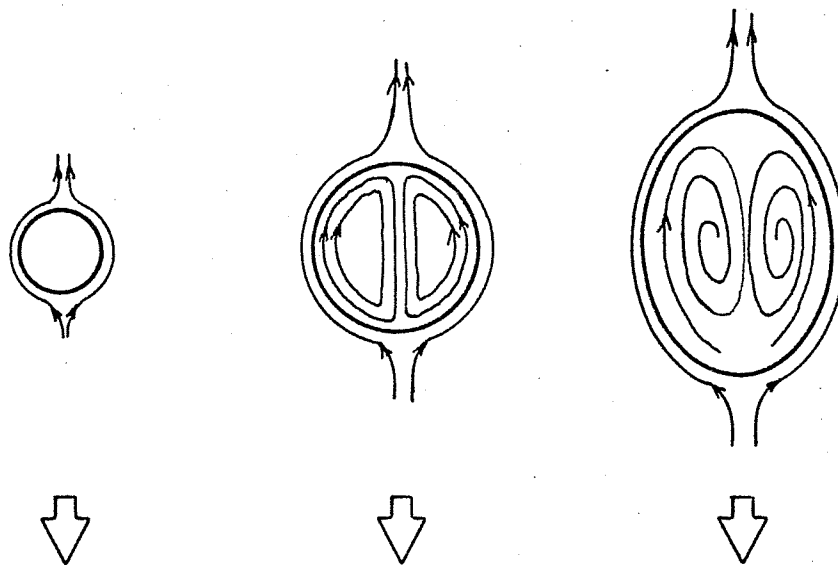
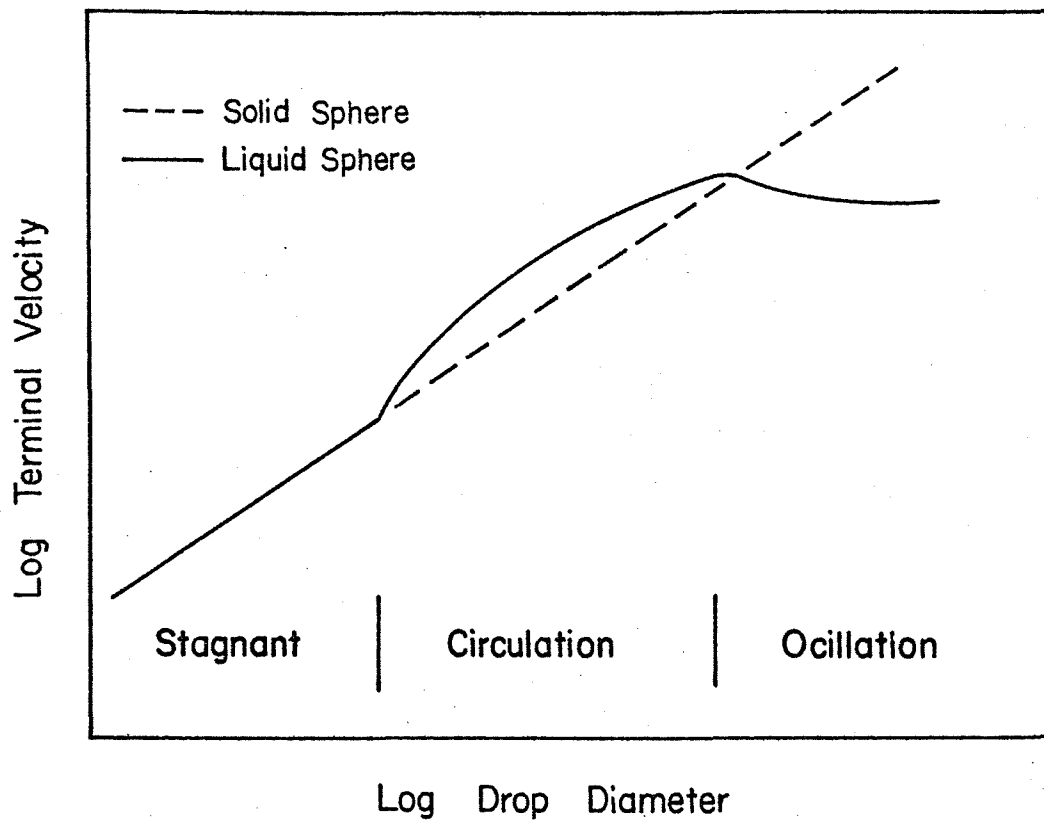


Figure 2. Terminal velocity and internal flow pattern for a liquid sphere as a function of drop diameter.

these circumstances the terminal velocity will be greater than that of the non-circulating drop, the solid sphere. As the drop size is increased to region C, the larger drop will travel at about the same speed, independent of size. Oscillation of the drop can be observed in this region and the internal flow pattern is a combination of eddy flow and circulation.

Viscosity, interfacial surface tension and the density difference will also influence the circulation of the liquid sphere. The amount of the circulation will be damped out in a viscous sphere even if the momentum can be transferred through the liquid-liquid interface. Hadamard⁽¹³⁾ has proposed a factor to correlate the terminal velocity of a circulating drop with the velocity of the non-circulating drop (solid sphere) as,

$$\frac{1}{k} = \frac{U_{t \text{ liquid}}}{U_{t \text{ solid}}} = \frac{3\mu_d + 3\mu_c}{3\mu_d + 2\mu_c} \quad (12)$$

For well circulating drops $1/k = 1.5$ and for non-circulating drops $1/k = 1.0$.

The surface tension reduces the circulation in such a way that it takes more energy to create the new surface at the front of the drop than to generate the circulation at the interface, and, as a result, the transport of momentum across the interface is diminished. Bond and Newton⁽¹⁴⁾ used dimensional analysis to study the effect of the surface tension and density difference on circulation in a liquid sphere. They defined a critical diameter at which complete circulation is established by the following equation,

$$d_c = 3\sqrt{\frac{g_c \sigma}{g|\rho_c - \rho_d|}} \quad (13)$$

Johnson and Braida⁽¹²⁾ tried to correlate several dimensionless groups which include density, diameter, viscosity and surface tension in order to predict the terminal velocity of drop. Drop oscillation can also be predicted from the correlation. However, the authors did not identify the conditions for transition from a stagnant drop to a circulating drop.

Internal Mass Transfer for Liquid Spheres

Due to the change in the internal flow pattern of the moving drop, internal mass transfer must also be evaluated in three different regions; the stagnant region, the circulation region and the oscillation region.

The mass transfer equation for a stagnant drop can be derived from the continuity equation based on Fick's 2nd law for which the transport depends only on molecular diffusion.⁽¹⁵⁾ By placing appropriate initial and final boundary conditions on the system, the dynamic expression for mass transfer in the stagnant drop can be obtained,

$$\frac{C_0 - \bar{C}_t}{C_0} = 1 - \frac{6}{\pi} \sum_{n=1}^{\infty} \frac{1}{n^2} \exp [-Dn^2 \pi^2 t/a^2] \quad (14)$$

where C_0 = initial concentration in dispersed phase

\bar{C}_t = average concentration in dispersed phase at time t

D = diffusion coefficient

a = drop radius

t = time

For short reaction times ($t < 40$ sec.), the integrated rate equation can be approximated by

$$\frac{C_0 - \bar{C}_t}{C_0} = \frac{\Delta C_t}{C_0} = 3.38 \left(\frac{Dt}{a^2} \right)^{1/2} \quad (15)$$

And the rate of transport in moles/sec can be written as

$$I = \frac{4}{3} \pi a^3 \frac{dc}{dt} = 7.08 C_0 a^2 \sqrt{\frac{D}{t}} \quad (16)$$

The mass transfer equation for a circulating drop is more complicated in that both molecular diffusion and convective transport must be considered. Kronig and Brink⁽¹⁶⁾ have derived a mass transfer equation using streamline functions (based on Hadamard circulation pattern) together with an expression for molecular diffusion from one streamline to another. The derived mass transfer equation is,

$$\frac{C_0 - \bar{C}_t}{C_0} = 1 - \frac{3}{8} \sum_{n=1}^{\infty} A_n^2 \exp \left[-\mu_n \frac{16Dt}{a^2} \right] \quad (17)$$

where μ_n = eigen values

A_n = function of eigen function

For short reaction times ($t < 25$ sec.), the equation can be simplified as

$$\frac{\Delta C_t}{C_0} = 4.65 \left(\frac{Dt}{a^2} \right)^{1/2} \quad (18)$$

And the rate of transport in moles/sec can be derived as

$$I = 9.73 C_0 a^2 \sqrt{\frac{D}{t}} \quad (19)$$

Due to the complexity of the internal flow pattern of the oscillating drop, there is no satisfactory model for internal mass transfer derived from first principles but some empirical equations exist.⁽¹⁷⁾ Drop oscillation occurs when the diameter of the drop is greater than 5 mm, a size which

generally is not of interest in solvent extraction systems. As a result, internal mass transfer for the oscillating drop will not be considered.

External Mass Transfer for Liquid Spheres

When the reaction rate is controlled by mass transfer in the continuous phase, the reactant species has to pass through the mass transfer boundary layer adjacent to the drop surface. Levich⁽¹⁸⁾ has derived a theoretical expression for mass transfer in the continuous phase. The rate of transport in moles/sec can be determined by the following equation,

$$I = 5.79 \left(\frac{\mu_c}{\mu_c + \mu_d} \right)^{1/2} \sqrt{DU/a} a^2 \Delta C_c \quad (20)$$

where μ_c, μ_d = viscosity of the continuous phase and dispersed phase, respectively

U = terminal velocity

ΔC_c = concentration gradient in the continuous phase.

Other investigators have used dimensional analysis to obtain empirical correlations, Skelland and Cornish⁽¹⁹⁾ for stagnant drops and Garner and Tayeban⁽²⁰⁾ for circulating and oscillating drops.

In order to assess the relative importance of external mass transfer and internal mass transfer, a comparison was made as shown in Figure 3 where the modified rate of transport (rate divided by the initial concentration of the diffusing species in the dispersed phase), is plotted as a function of the drop travel time. Figure 3 was constructed by using the stagnant model for internal mass transfer and the Levich equation for external mass transfer. A family of curves for several initial concentration

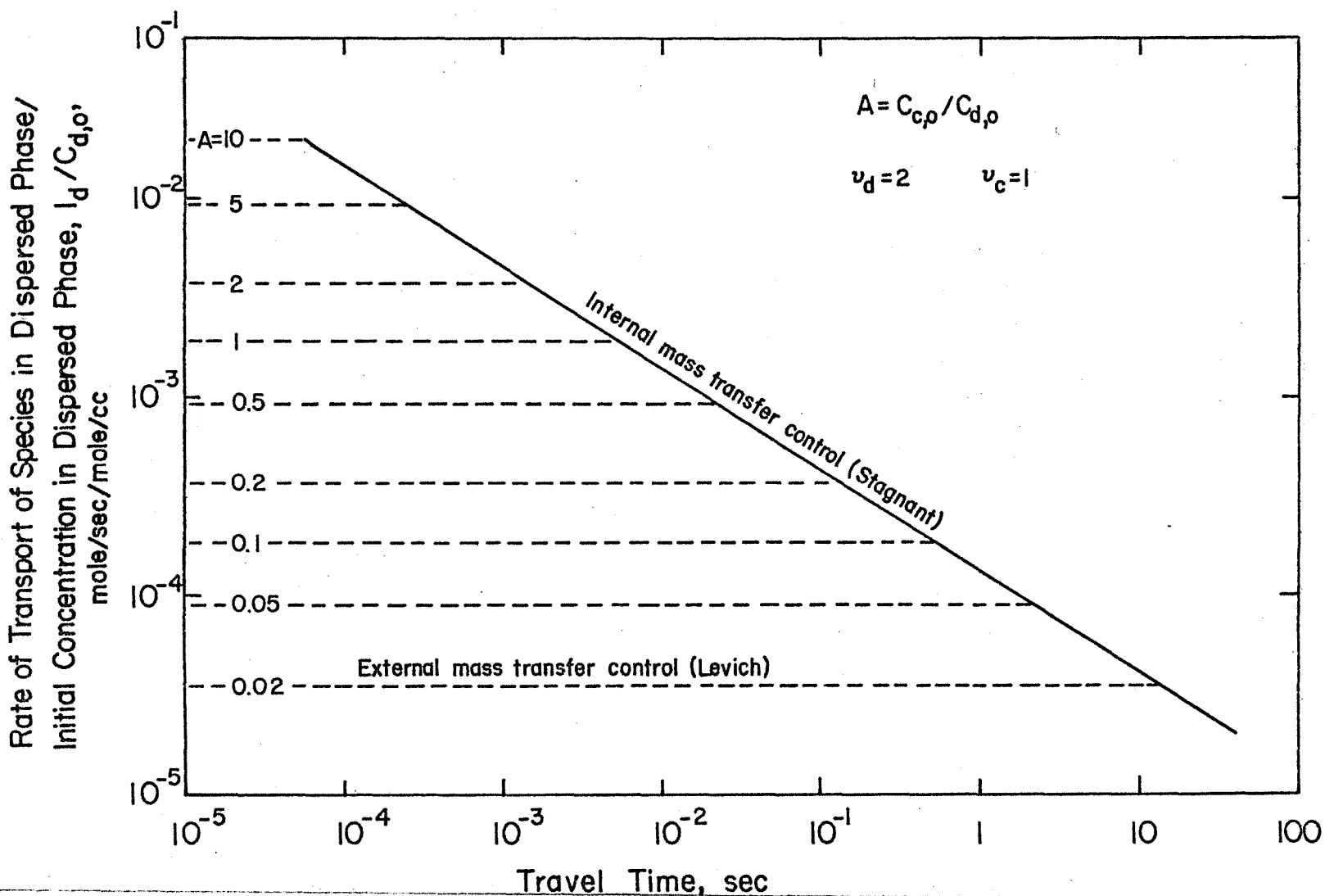


Figure 3. Representation of the relative importance of transport processes in the continuous and in the dispersed phase for various reactant concentration ratios. Intersection of horizontal dashed line with diagonal line indicates the critical time (t_c) during which the rate is limited by mass transfer in the continuous phase.

Conditions: $D_c = 7.5 \times 10^{-6}$ cm²/sec, $D_d = 4 \times 10^{-6}$ cm²/sec, $a = 0.1$ cm.

$\mu_c = 1$ cp

$\mu_d = 1.68$ cp, $v = 10$ cm/sec, $v_d = 2$, $v_c = 1$ ($v =$ stoichiometric number).

ratios, $C_{c,0}/C_{d,0}$, is shown,

where $C_{c,0}$ = initial concentration of continuous phase reactant

$C_{d,0}$ = initial concentration dispersed phase reactant.

The plot indicates that the rate is controlled by external mass transfer initially and is then taken over by internal mass transfer after some critical time, t_c , which depends on the initial concentration ratio. The time interval when the reaction rate would be controlled by external mass transfer is too small to be significant unless the initial concentration ratio is smaller than 0.05. This implies that in normal solvent extraction systems external mass transfer is faster than internal mass transfer so that generally, external mass transfer will not be rate limiting.

Chemical Reaction at the Interface

Under certain circumstances it is possible that transport processes will be rapid compared to chemical reaction and under these circumstances the rate will be determined by the intrinsic reaction kinetics associated with the reaction mechanism. However, it is generally impossible from available physico-chemical evidence alone to establish with certainty the location of the rate-controlling step in the chemical reaction. Thus, detailed kinetic studies are necessary to establish coefficients for empirical rate expressions with complex reaction order,

$$\text{Rate} = k_f \pi C_i^{v_i} - k_r \pi C_j^{v_j} \quad (21)$$

where k_f, k_r = rate constants of forward and backward reaction, respectively

C_i, C_j = concentrations of reactants and products, respectively

v_i, v_j = reaction orders of reactants and products, respectively.

Drop Size Distribution in the Mixer^(21,22,23)

The pertinent variables that control the drop size distribution in a liquid-liquid extraction mixer are: (1) impeller type; (2) impeller speed; (3) system geometry; and (4) the physical properties of the liquids and their volume ratio.

Impellers are classified according to the type of flow patterns and the methods of discharge that they produce. Essentially there are three major types of impeller; marine, turbine and paddle. Marine impellers are designed to product primarily an axial flow of fluid. Turbine impellers give a radial flow of fluid. Paddle impellers are generally slow moving. They push the liquid in front of them and thus produce primarily a tangential flow pattern. The three major impellers and the flow they generate are represented in Figure 4. The impeller type, blade size, width, angle and number of blades are important variables that can influence the performance significantly. These factors affect the nature of the breakage mechanisms and the circulation frequency within the vessel which will specify the drop size distribution.

The second important variable in the mixer is the impeller speed which reflects the power input into the system. The speed of the impeller tip is the most influential factor on drop size.

The geometry of a mixer can have an appreciable effect on droplet size and especially on the power consumption. Included in this area are such functions as the ratio of the impeller diameter to the tank diameter, D/T , the position and number of impellers and the effects of baffling. The D/T ratio is generally considered to have little influence on system in

FLOW PATTERN

IMPELLER TYPE

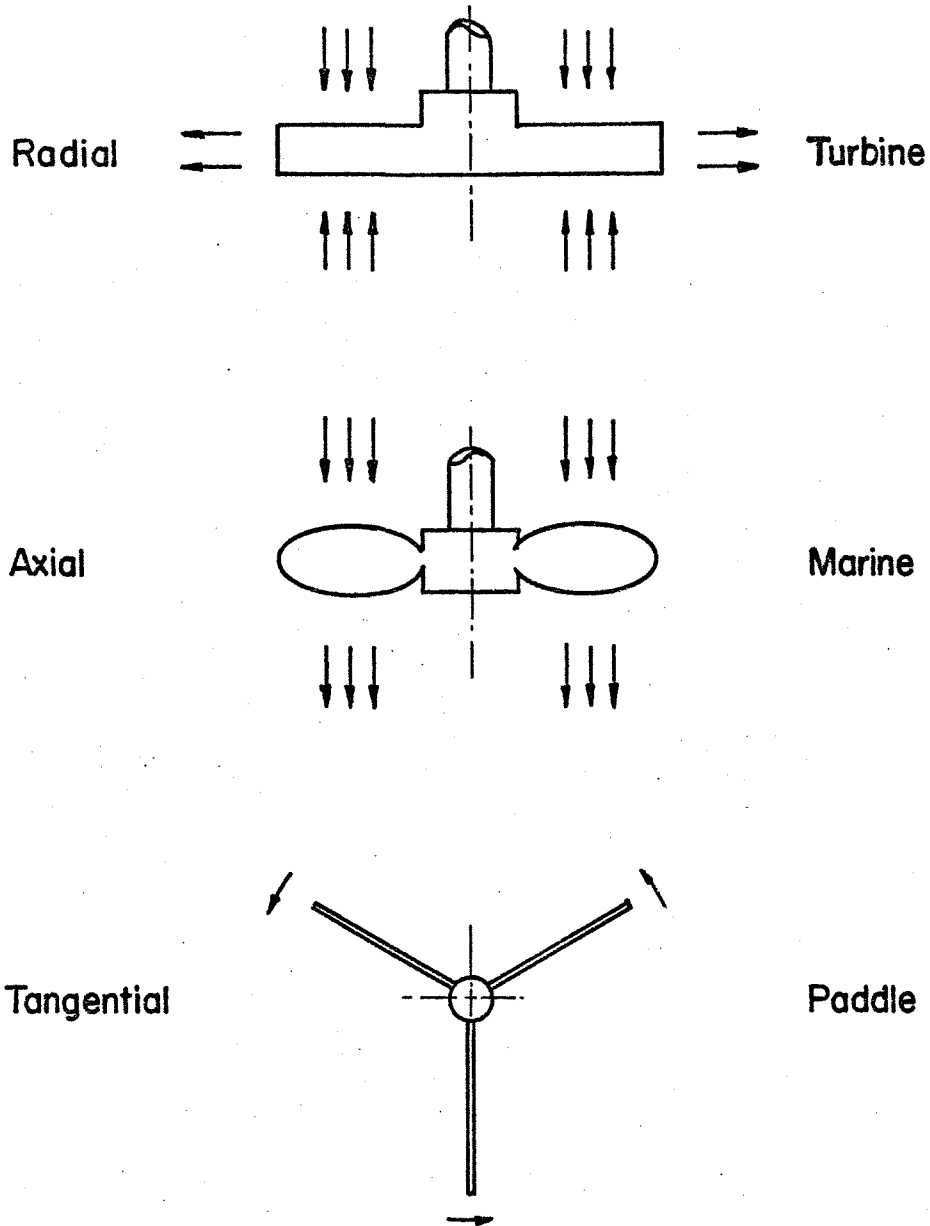


Figure 4. Classification of Impellers by their flow pattern.

the range of 0.15 to 0.5. Normally, impellers are positioned $1/2$ to $2/3$ of the liquid distance to the bottom of the vessel to minimize the circulation time and ensure complete mixing of the heavy phase.

The final major parameter affecting droplet size is that of the physical properties of the liquids and their phase ratio. Generally the influence of physical properties is only significant at low speeds and power input. The drop size distribution becomes coarser as the phase fraction of dispersed phase increases.

EXPERIMENTAL

The research program on copper extraction from ammoniacal solution has been divided into three major sections: the equilibrium study; the kinetic study and the drop size distribution in a mixer. The experimental approach was to identify the important variables in each section to provide fundamental information for further application.

Materials

The primary extractant for this study was LIX 64N provided by General Mills (lot no. 3K19304), the reagent was used without further purification. The organic diluent was Escaid 200 which has less than 1% aromatic component.

Other chemicals used in this research were reagent grade.

Stoichiometry of Extraction

The chemistry of copper extraction from ammoniacal solution was investigated by using the shake-out test. The organic solution, LIX 64N in Escaid 200, was shaken in a separatory funnel with an aqueous solution containing copper and ammonia from which the extraction was to be made. After about 30 minutes of vigorous shaking on the wrist shaker the phases were allowed to separate. Each phase was analyzed for copper by atomic absorption; for the aqueous phase, the amount of free ammonia had to be neutralized by sulfuric acid, and for organic phase the copper was stripped out with an aqueous sulfuric acid solution. The results were used to calculate the distribution coefficient and the amount of copper loaded in organic phase.

Extraction Kinetics

The kinetic study was carried out in a single drop reaction cell (SDRC). The apparatus consists of a reaction cell, orifice for drop formation, provision for drop removal, and temperature controller. A schematic diagram of the apparatus is shown in Figure 5. Depending on the density difference of the dispersed phase and the continuous phase, the data can be collected either for a falling drop or a rising drop. After the dispersed phase was selected, the solution was introduced from the head tank to the reaction cell. For organic dispersed experiments, the organic drops were formed at the bottom of the cell from the syringe needle. After rising through the cell, the drop coalesced at the top of the aqueous/organic interface, and discharged through a tube being collected outside the cell. For aqueous dispersed experiments, the system was reversed, and the aqueous drops allowed to fall through the cell. The size of the drop can be varied by using needles with different size openings. By controlling the head pressure, a constant frequency of droplet generation can be obtained which usually is in the range of 80 to 100 drops per minute. The drop rate should be maintained as constant as possible, because variation in the drop rate may influence the mass transfer that occurs at the ends of the cell during drop formation and coalescence periods (end effects), which makes data interpretation more difficult. The average drop size can be calculated from the number of drops required to collect a specific volume. The contact time during the steady state travel is measured by timing the travel of a drop from the tip of the needle to the coalescence interface. The travel time can be varied by changing the length of the cell which ranged from 20 to 160 cm.

- A : Dispersed phase reservoir
- B : Temperature controller
- C : Head Tank
- D : Reaction Cell
- E : Syringe needle
- F : Continuous phase
- G : Volumetric
- H : Oil bath
- I : Pump

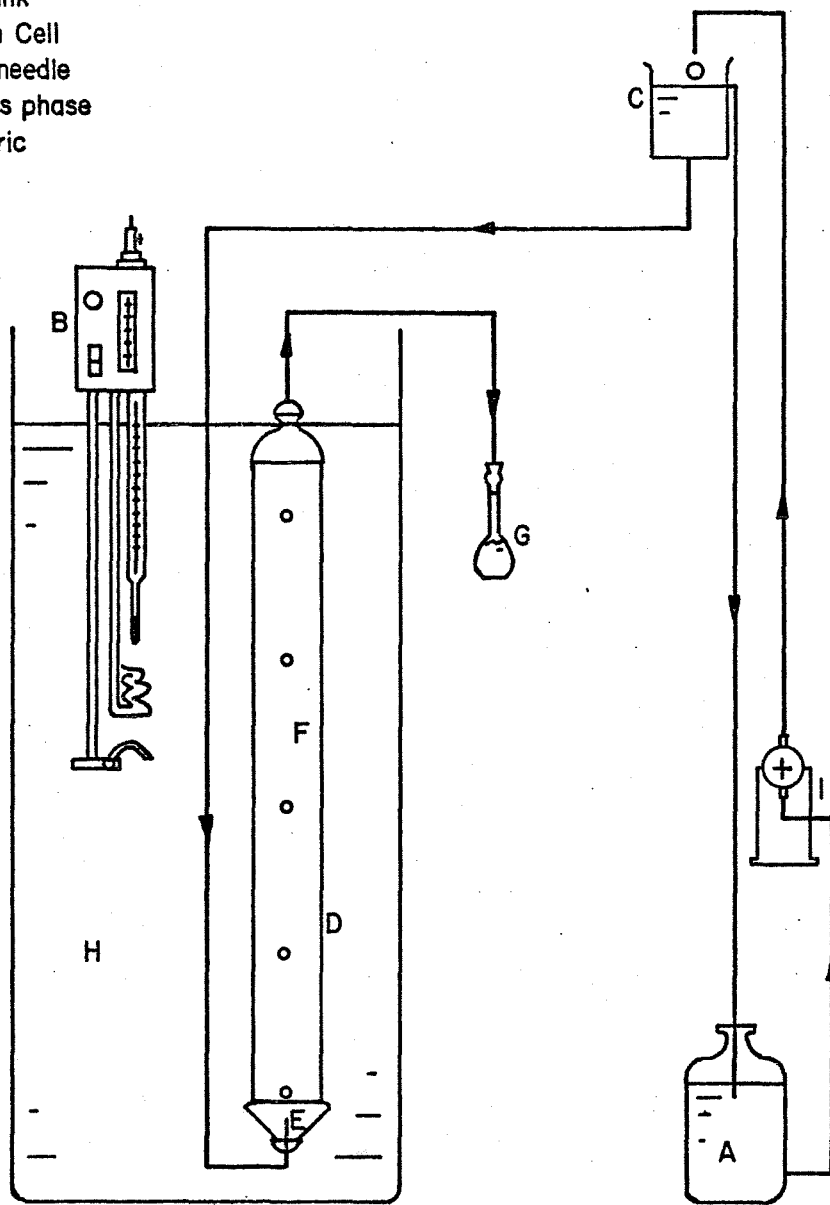


Figure 5. Schematic diagram of Single Drop Reaction Cell (SDRC).

The amount of copper extracted or amount of LIX 64N reagent consumed for each experiment was determined by measuring the copper concentration with an atomic absorption spectrophotometer (the same method as used in the equilibrium study).

In this study, the experiments were designed so that the kinetics of extraction could be investigated when the drops were organic phase (rising drop) or when the drops were aqueous solution (falling drop). The data were analyzed to determine the effect of copper concentration in the aqueous solution, the effect of LIX 64N concentration in organic phase, the effect of different drop sizes, the effect of different contact times and the effect of different temperatures. The results were analysed in terms of the theoretical considerations associated with mass transfer in moving drop systems.

Droplet Size Determination in a Mixer

Agitation Equipment

Two different agitators have been used to study drop size distribution. The first is the Benco ELB Experiment Agitation kit with dynamometric accessories. This unit consists of a standard 1/4 hp drive motor and transmission, which allows for speeds from 0 to 1100 rpm, mounted on a dynamometer stand with a torque meter for power input measurements. The kit comes with a variety of marine and turbine impellers. To obtain information on the behavior of smaller drop sizes another agitator was used which consists of an enclosed 4.6 liter steel vessel mounted on a steel stand for stability and agitated by means of a hydraulic pump drive assembly

which allows speeds in excess of 5000 rpm. The schematic diagram of the agitation vessel is shown in Figure 6.

Range of Operation

The equipment described above permits a good deal of flexibility in the investigation of liquid-liquid systems. However, most experiments were run in the batch mode with vessels of approximately the same size (1.0-1.6 gallons) and a few with larger vessels of about 5 gallons. The ratios of impeller size to tank diameters (D/T) ranged from .33 to .67 with .4 being the most extensively studied. All tests were made with flat blade turbine impellers.

Speeds in the range of 400 rpm to 3500 rpm were investigated with most work being concentrated at the higher speeds. The ratios of organic to total liquid phases (phase fraction) investigated were generally between .10 and .40 with some lower phase fractions investigated for photographic purposes.

Droplet Size Measurement

Two methods of measuring drop sizes were developed in this work. The first employs the principle of gelatin embedding to 'freeze' the drops in a gelatin matrix where they can be counted. This method utilizes a 8% solution of pig skin gelatin at a temperature of 30°C. Approximately 5 cc of this solution is placed in a small test tube and about 0.5 cc of emulsion is withdrawn carefully from the mixer and immersed in the gelatin solution. This solution is then poured rapidly on to a petri dish and manipulated to give an uniform, smooth layer on the bottom. The sample is

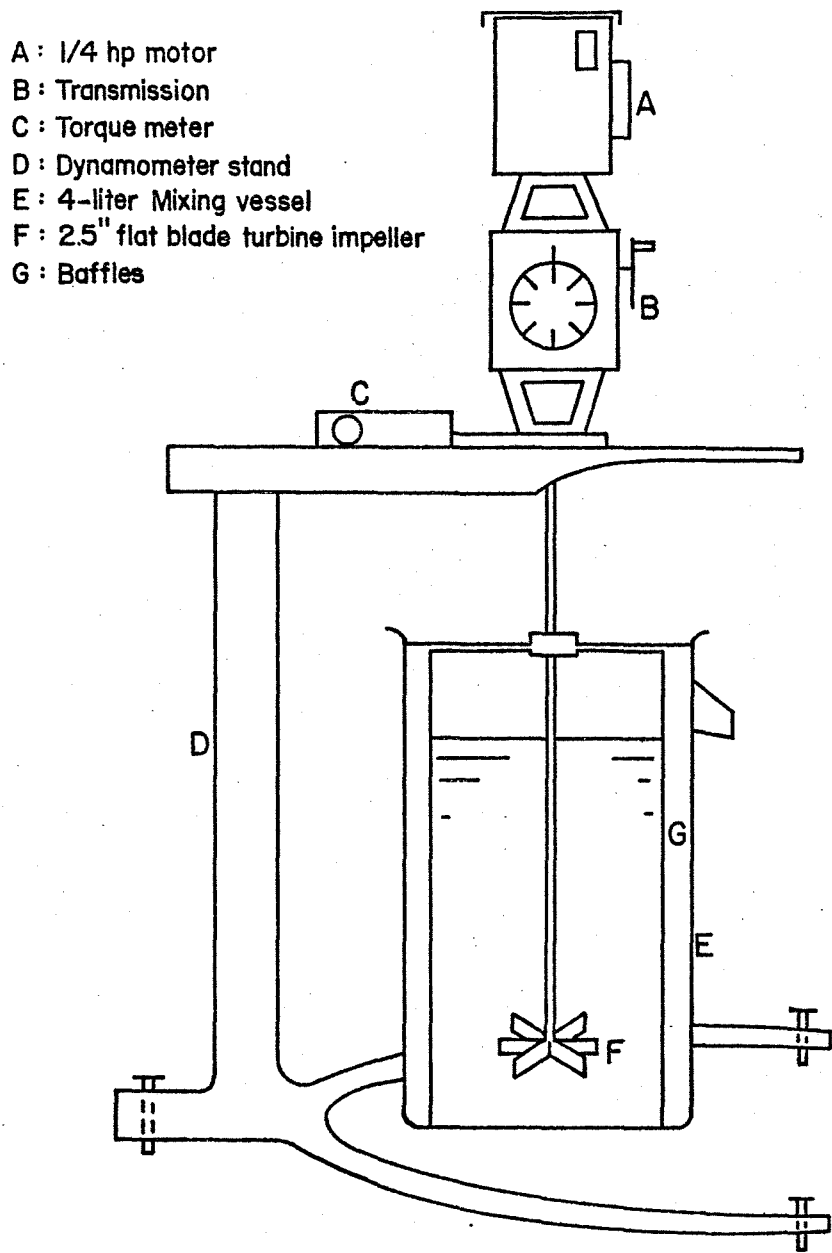


Figure 6. Schematic diagram of agitation vessel.

then cooled rapidly to set the gelatin. The resulting sample must then be analyzed by counting the drops under a microscope or by more sophisticated equipment if available.

The second method of size measurement involves the principle of microencapsulation by an interfacial polycondensation reaction. This reaction takes place when an acid chloride comes in contact with a diamine to produce a polymer and acid as a byproduct.

The technique as applied here consists of placing sebacyl chloride of .04 molar concentration in the organic phase and agitating this with the aqueous phase for the desired amount of time. A sample of emulsion (20-25 cc) is then siphoned out of the mixer where it is combined with an equal amount of diamine solution. The diamine solution contains .036 molar hexamethylene-diamine and .004 molar 4,4'-diamino 2,2'-diphenyldisulfonic acid in a .45 molar $\text{NaHCO}_3\text{-Na}_2\text{CO}_3$ buffer solution. The polymer film is formed at the interface of the droplet encapsulating the organic.

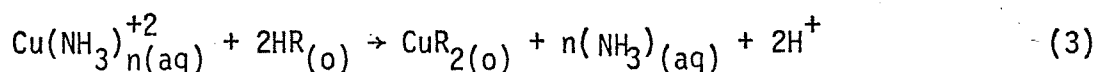
After mixing briefly to strengthen the drops they are ready for analysis which can be accomplished by a number of methods. If the drops are under 200 microns in size they can be analyzed by the Leeds & Northrup Particle Size Analyzer which utilizes light scattering principles to measure the distribution. The Coulter Counter Model TA has also been used to count and size encapsulated drops and can be used over a variety of size ranges if the proper apertures are available.

RESULTS AND DISCUSSION

Equilibrium Study

It has been reported that the copper extraction by LIX 64N in acidic media involves a complete displacement of the coordinated water molecules of the cupric ion by LIX 64N extractant. In this study an infrared spectrophotometric analysis was used in order to compare the extracted complex of copper from the ammoniacal solution with that from the acidic solution. The results, shown in Figure 7, indicate that the extracted complex is identical for both systems and suggest that copper extraction from ammonia solution also involves complete displacement of coordinated ammonia ligands. Otherwise, the extracted complex should have a primary absorption band near 3300 cm^{-1} for any ammonia molecules retained by the complex. The absorption near 2500 cm^{-1} is due to the absorption of the silica cell. In addition, Kjeldahl analysis for ammonia showed that the organic phase contained a negligible quantity of ammonia.

From the above findings, the chemical reaction can be written as,



and the extraction coefficient can be presented as

$$\log E = \log K - \log \left(1 + \sum_1^6 \beta_i [\text{NH}_3]^i \right) + 2 \log [\text{HR}]_{(o)} + 2\text{pH} \quad (6)$$

Effect of Free Ammonia

Figure 8 shows the effect of free ammonia concentration on copper extraction at a constant pH (10.2-10.5) which was maintained by keeping the ratio of $[\text{NH}_3]_{\text{free}}/[\text{NH}_4^+]$ constant at 2:1. The system had an excess amount

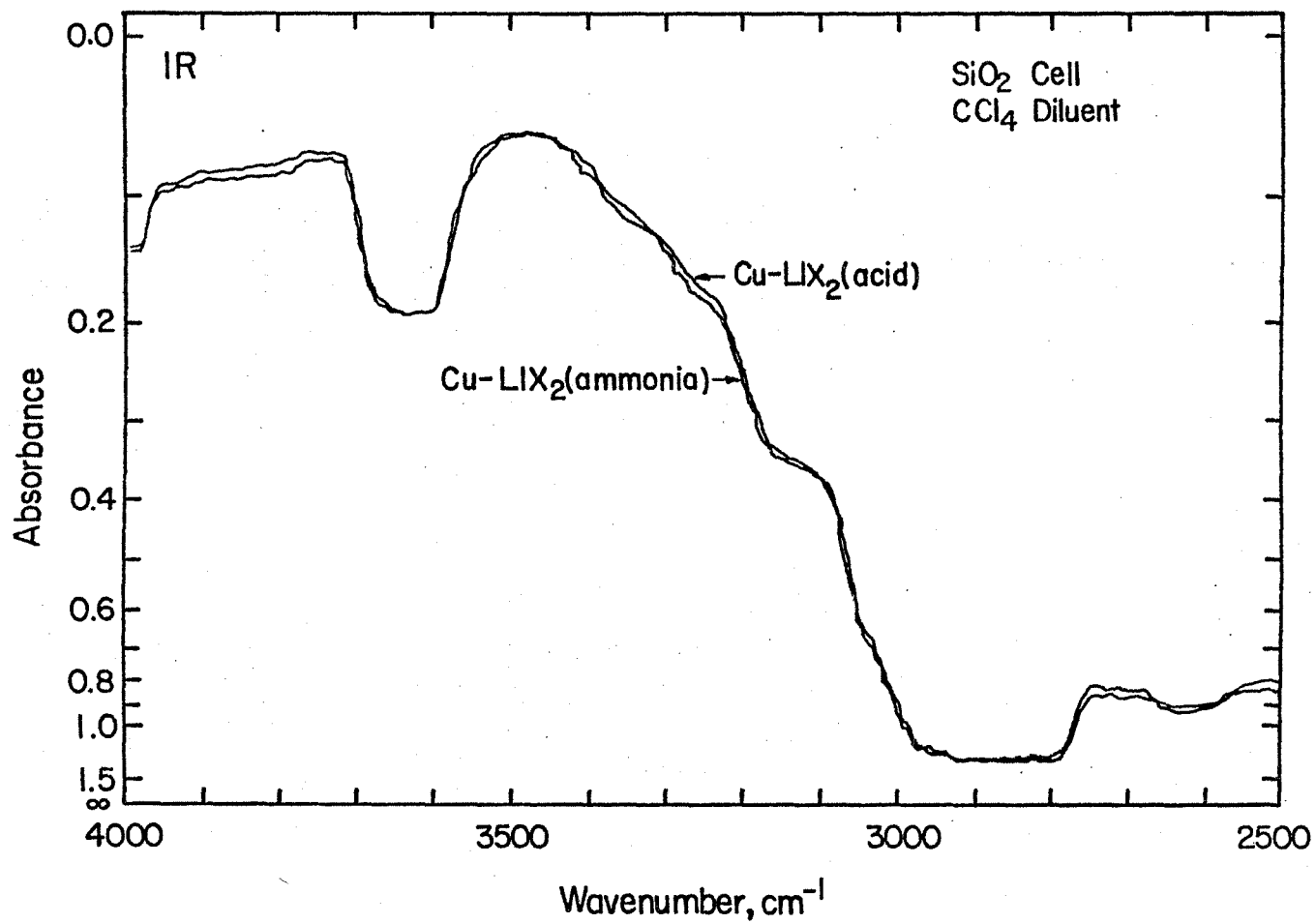
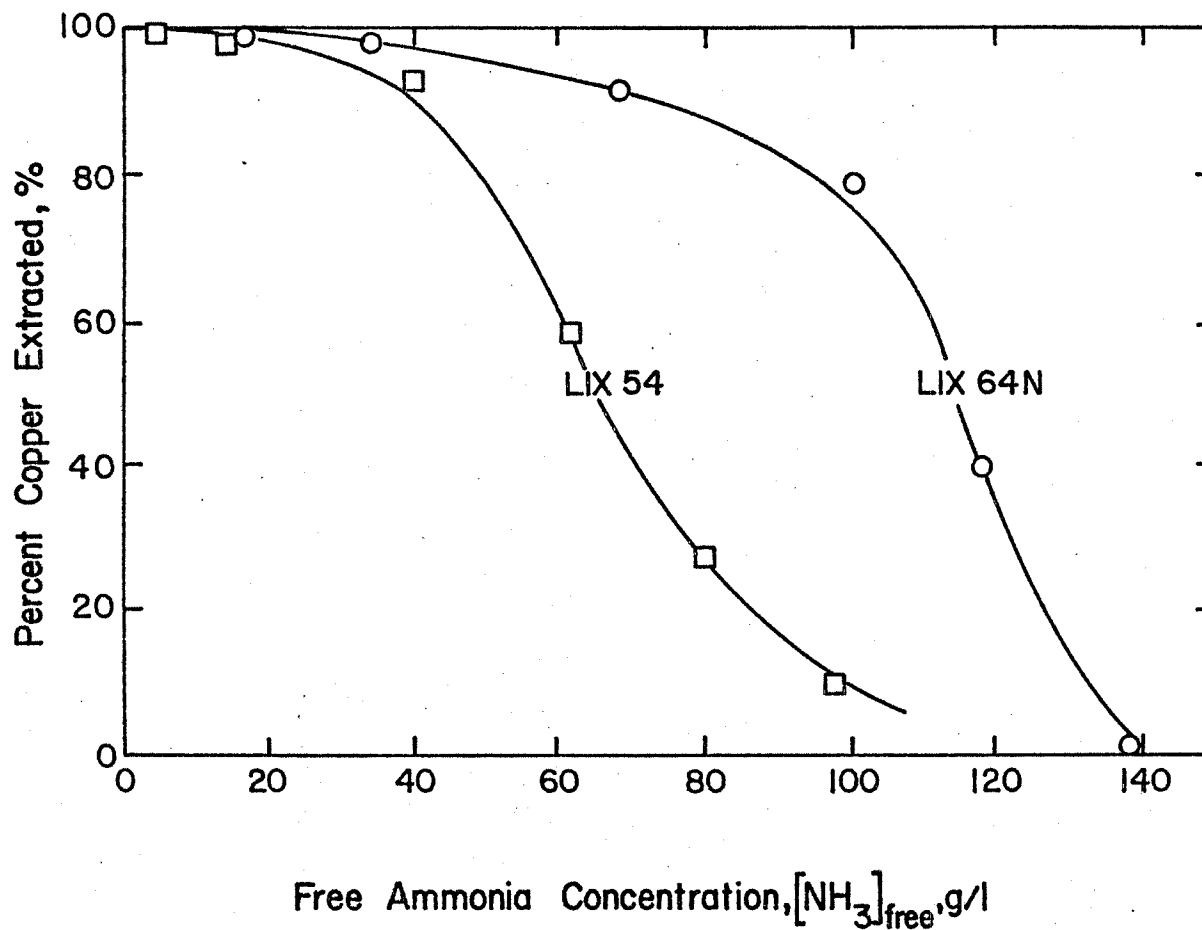


Figure 7. IR spectra of organic phase obtained from both acidic and ammoniacal solutions.



LIX 64N: 0.004M Copper; 40% LIX 64N in Escaid 200; A/O 1:1; $\text{NH}_3/\text{NH}_4^+$ 2:1
 LIX 54: 0.005M Copper; 38% LIX 54 in Cyclosol 63, A/O 1:1; $\text{NH}_3/\text{NH}_4^+$ 2:1

$$\log E = \log K - \log(1 + \sum \beta_i [\text{NH}_3]^i) + 2\text{pH} + 2\log[\text{HR}]_0$$

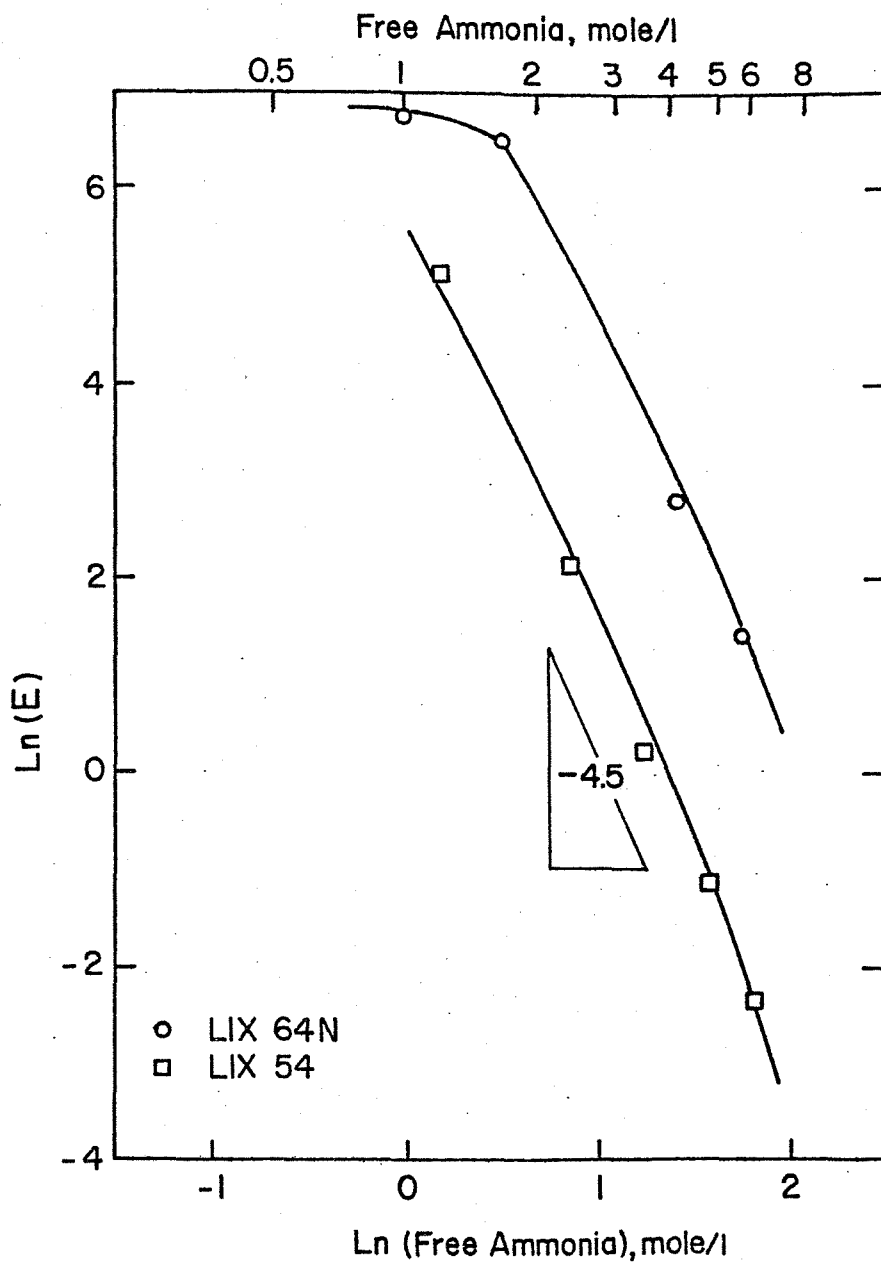
Figure 8. Effect of ammonia concentration on copper extraction at constant pH (10.2-10.5).

of extractant and a small amount of copper, so that the concentration of the extractant can be considered to be constant, and the amount of coordinated ammonia can be neglected. As expected from the extraction coefficient equation, Equation 6, the results show that the copper extraction decreases as the ammonia concentration increases for both LIX 64N and LIX 54 (β -diketone). The LIX 64N extractant seems to form a more stable copper complex than LIX 54 in the ammoniacal solution.

According to Equation 6, a plot of $\log E$ vs: $\log [\text{NH}_3]_{\text{free}}$ should be indicative of the number of coordinated ammonia molecules. Figure 9 is such a plot and the average slopes for both extractants is seen to be 4.5. This suggests that the cupric ion in ammoniacal solution is coordinated by an average of 4 to 5 ammonia molecules which is in good agreement with the value that would be predicted from the stability constants for copper-ammine complexes (Equation 4).

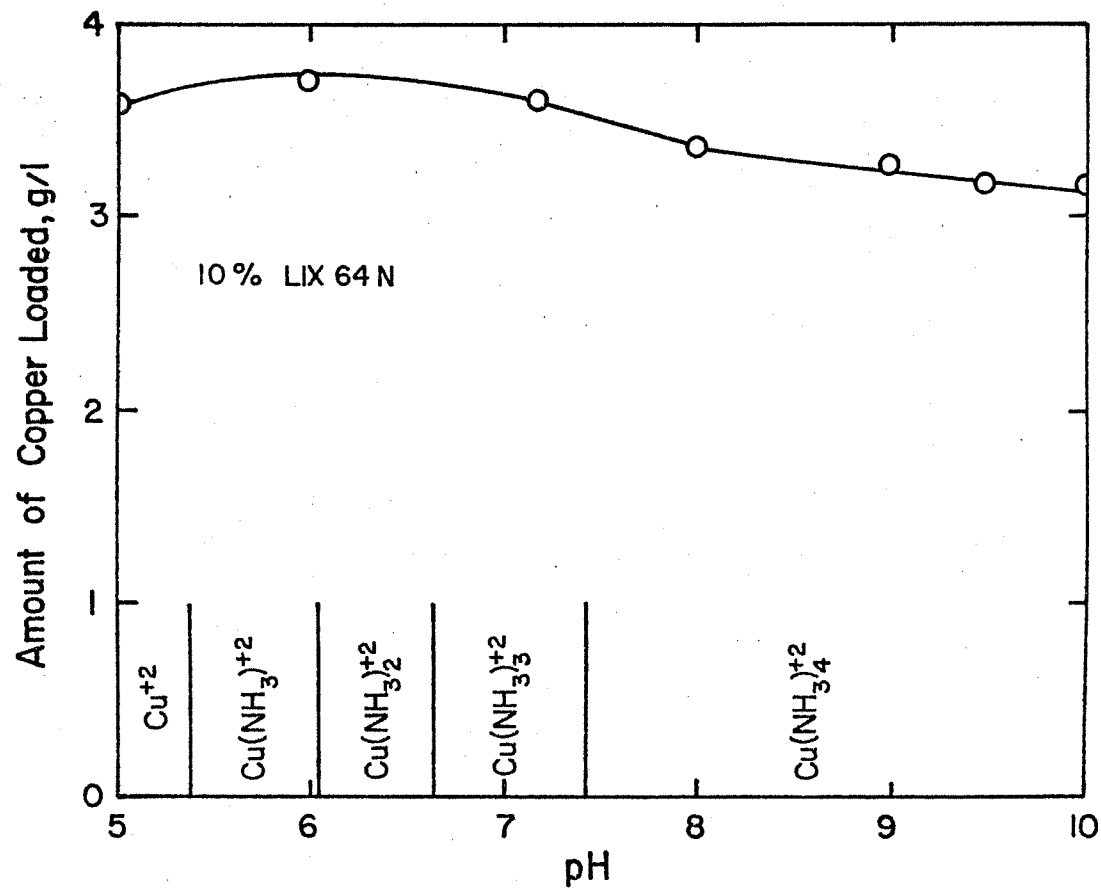
Effect of pH

The effect of the pH on copper extraction was performed by keeping the total amount of ammonia, $[\text{NH}_3]_{\text{free}}$ plus $[\text{NH}_4^+]$, constant at 0.5 M. In this case, the extraction of copper is more complicated due to the fact that the pH value has a positive effect on extraction while free ammonia concentration has a negative effect, shown by Equation 6. As a result, a parabolic-type of curve is obtained for a plot of copper extraction as a function of pH. See Figure 10. For low pH values, copper extraction increases as the pH increases, which may be due to the pH effect only, because the concentration of free ammonia is negligibly small at these low pH values. However, at high pH values (above the maximum loading



$$\log E = \log K - \log(1 + \sum \beta_i [\text{NH}_3]^i) + 2\text{pH} + 2\log[\text{HR}]_0$$

Figure 9. Slope Analysis plot indicative of the number of ammonia molecules coordinated by the cupric ion under the conditions specified in Figure 8.



$$\log E = \log K - \log(1 + \sum \beta_i [\text{NH}_3]^i) + 2\text{pH} + 2\log[\text{HR}]_0$$

Figure 10. Effect of pH on copper extraction at a constant total ammonia concentration of 0.5 M.

at pH 6 in Figure 10), the concentration of the ammonia and the number of ammonia ligands will be increased significantly. In this region the ammonia effect will overcome the pH effect and the copper extraction will diminish. This behavior has also been found in the extraction of nickel from the ammoniacal solution. (24)

Kinetic Study

The kinetics was studied in both rising drop and falling drop experiments. The results were used to analyze the effect of the drop size, the temperature and reagent concentrations both in dispersed phase and in continuous phase. By considering all the effects, the rate controlling step was proposed to be reactant mass transfer in the dispersed phase and a comparison between the experimental results and theoretical predictions was made. Normally, the organic phase consisted of the diluent Escaid 200 and the extractant, LIX 64N (50% active) with no copper loaded initially. The copper concentration in the aqueous phase ranged from 0.5 to 5.3 g/l with 1 M total ammonia (0.5 M free ammonia) at a pH of 9.75. The drop size was varied from 0.084 to 0.152 cm in radius.

Rising Drop Experiments

In this series of experiments the continuous phase was always the ammoniacal solution of copper sulfate, and the dispersed phase (drop) was the organic solution (LIX 64N in Escaid 200) containing no copper initially. The amount of copper extracted into the organic solution is related to the change in the LIX concentration by the stoichiometry of the reaction,

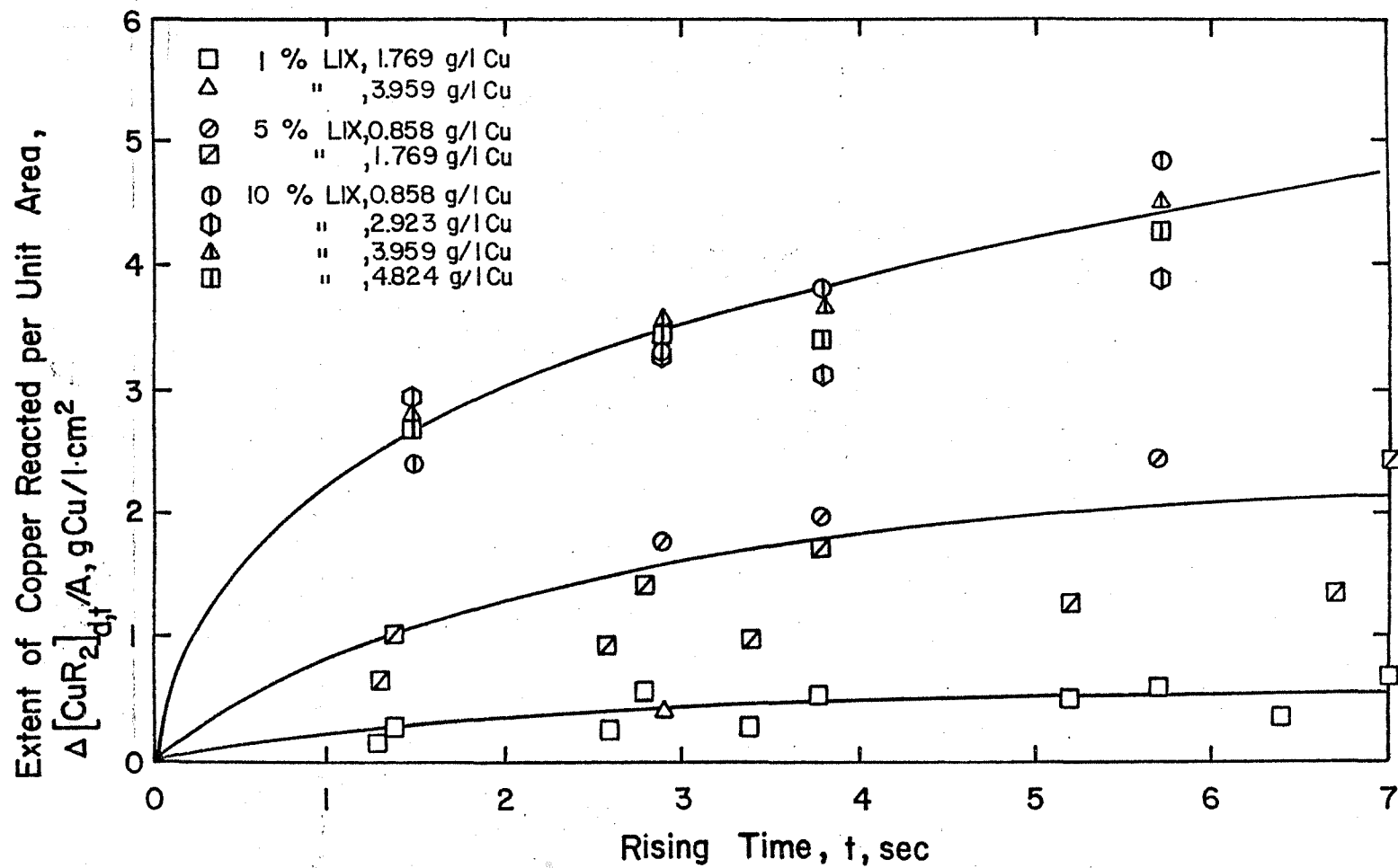


Figure 11. Rate of copper extraction into rising drops for various dispersed (organic) and continuous (aqueous) phase concentrations.

$$-\Delta[\text{HR}]_{d,t} = 2 \Delta[\text{CuR}_2]_{d,t} \quad (22)$$

which, since copper in the continuous aqueous phase is in considerable excess, can be transformed to,

$$-\Delta[\text{HR}]_{d,t} / [\text{HR}]_{d,0} = \Delta[\text{CuR}_2]_{d,t} / [\text{CuR}_2]_{d,\infty} \quad (23)$$

where $-\Delta[\text{HR}]_{d,t}$, $\Delta[\text{CuR}_2]_{d,t}$ = change in concentration of LIX and Cu in dispersed organic phase at time, t , respectively,

$[\text{HR}]_{d,0}$ = initial LIX concentration in dispersed organic phase,

$[\text{CuR}_2]_{d,\infty}$ = maximum copper loading in dispersed organic phase.

All data from rising drop experiments are represented by open symbols.

Effect of reactant concentration. Experimental results for two drop sizes with several concentrations of LIX 64N in the dispersed organic phase and several concentrations of copper in the continuous aqueous phase are presented in Figure 11. Because the reaction is directly proportional to the interfacial area, Figure 11 was plotted in terms of extent of copper reacted per unit area versus the travel time of the drop. Consideration of the experimental conditions where $[\text{HR}]_{d,0} / [\text{CuR}_2]_{c,0}$ ranged from 10 to 0.22, in terms of the analysis presented in Figure 3, suggests that rate control by external mass transfer should not be important under these conditions and that internal mass transfer would limit the rate for a fast surface reaction. The experimental results seem to support this argument. First, the rate is largely independent of copper concentration in the continuous phase, but distinctly dependent on the LIX 64N concentration in the dispersed phase. Second, the rate curves are parabolic in shape which would be expected for rate control by internal mass transfer. See equations 15 and 18.

More experimental data are provided in Figure 12 in which the extent of extraction is plotted vs. a parabolic scale corrected for changes in area,

$$-\Delta[\text{HR}]_{d,t} = k[\text{HR}]_{d,0} D^{1/2} \sqrt{t/a^2} \quad (24)$$

A linear relationship can be found for all concentrations of LIX 64N. Figure 12 also indicates that the end effects during the drop formation and drop coalescence are negligibly small which has been observed in several other systems. (25,26)

The reaction order with respect to the LIX 64N concentration in the dispersed phase can be determined from Equation 24,

$$-\Delta[\text{HR}]_{d,t} / \sqrt{t/a^2} = k[\text{HR}]_{d,0}^n$$

or

$$\ln[\text{Rate}] = \ln k + n \ln[\text{HR}]_{d,0} \quad (25)$$

The reaction order plot presented in Figure 13 indicates that the rate has a 1st order dependence on the LIX concentration and zero order dependence on the copper concentration. These results suggest that the kinetics of extraction are limited by internal mass transfer. The apparent deviation from this first order relationship at low LIX concentration is attributed convective transport and will be discussed later.

Effect of temperature. The internal mass transfer hypothesis is also supported by the low temperature coefficient observed from the data presented in Figures 14 and 15. Figure 14 shows that the kinetics of copper extraction increases as the temperature increases. It also shows

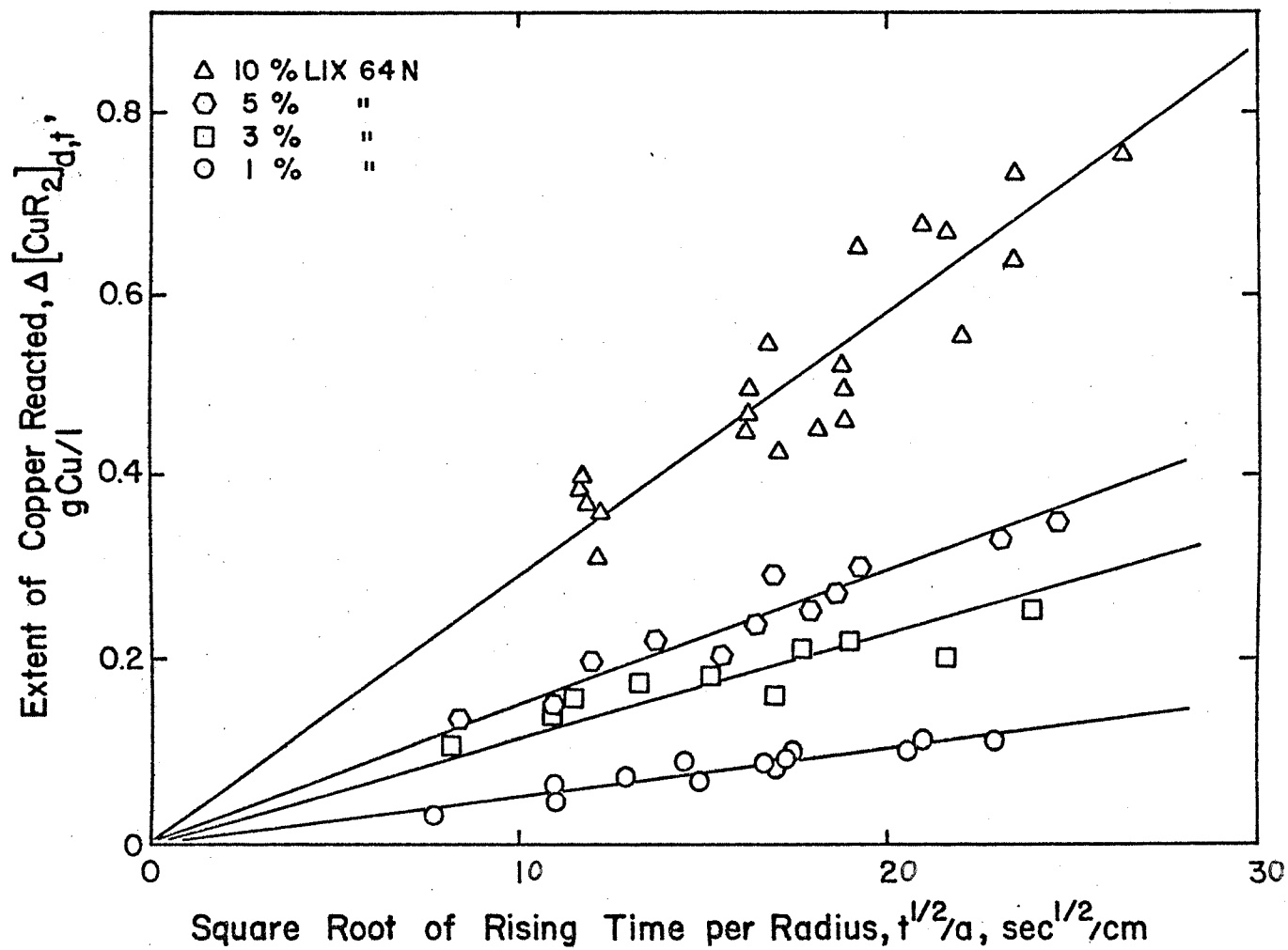


Figure 12. Parabolic plot of rate data illustrating that the kinetics conform to the linear relationship required for rate control by internal mass transfer.

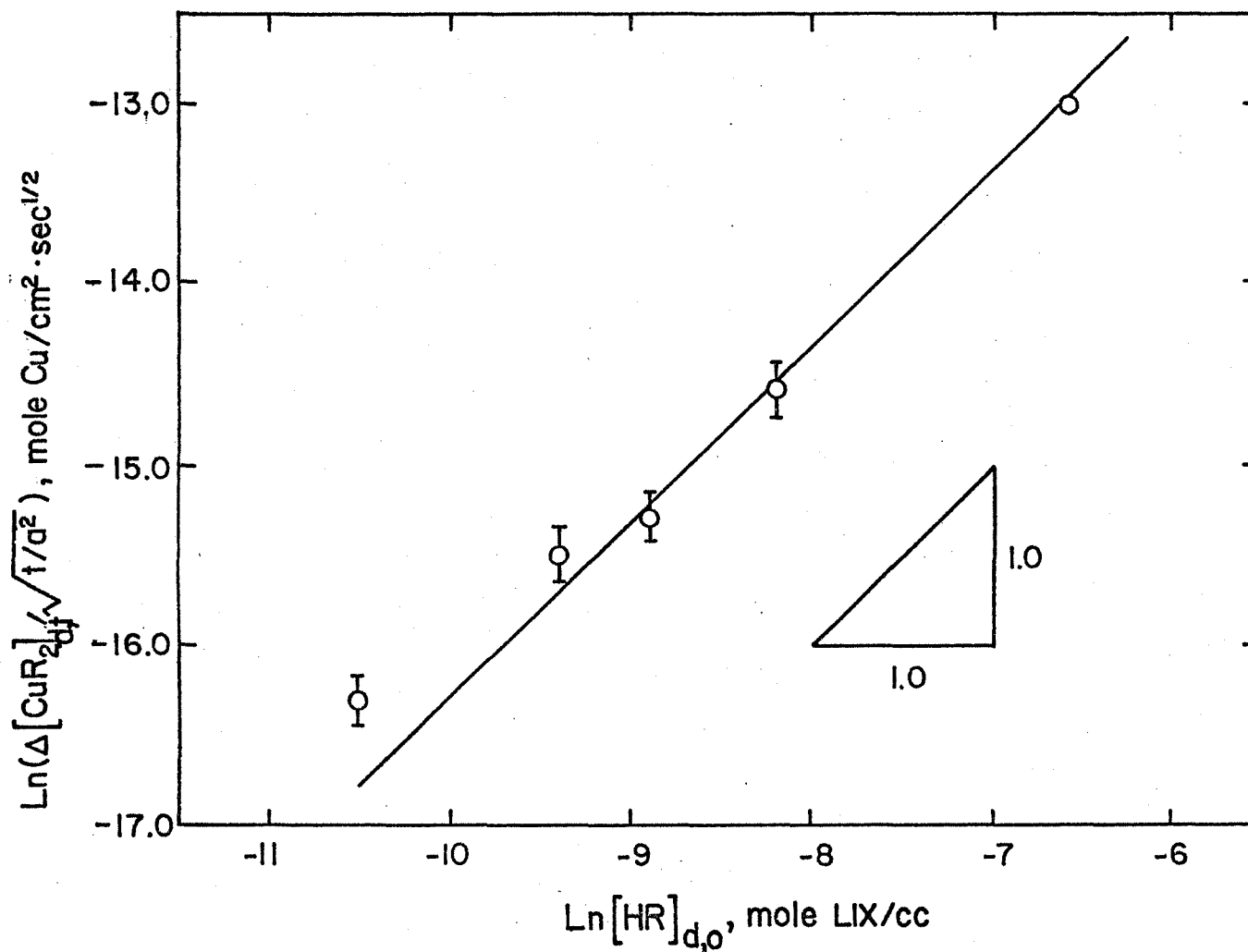


Figure 13. Reaction order plot illustrating the first order dependence on the extractant concentration in the dispersed phase. Vertical bars indicates the range of the rate for all the copper concentration in the continuous phase. Note that the rate is independent of copper concentration in continuous phase.

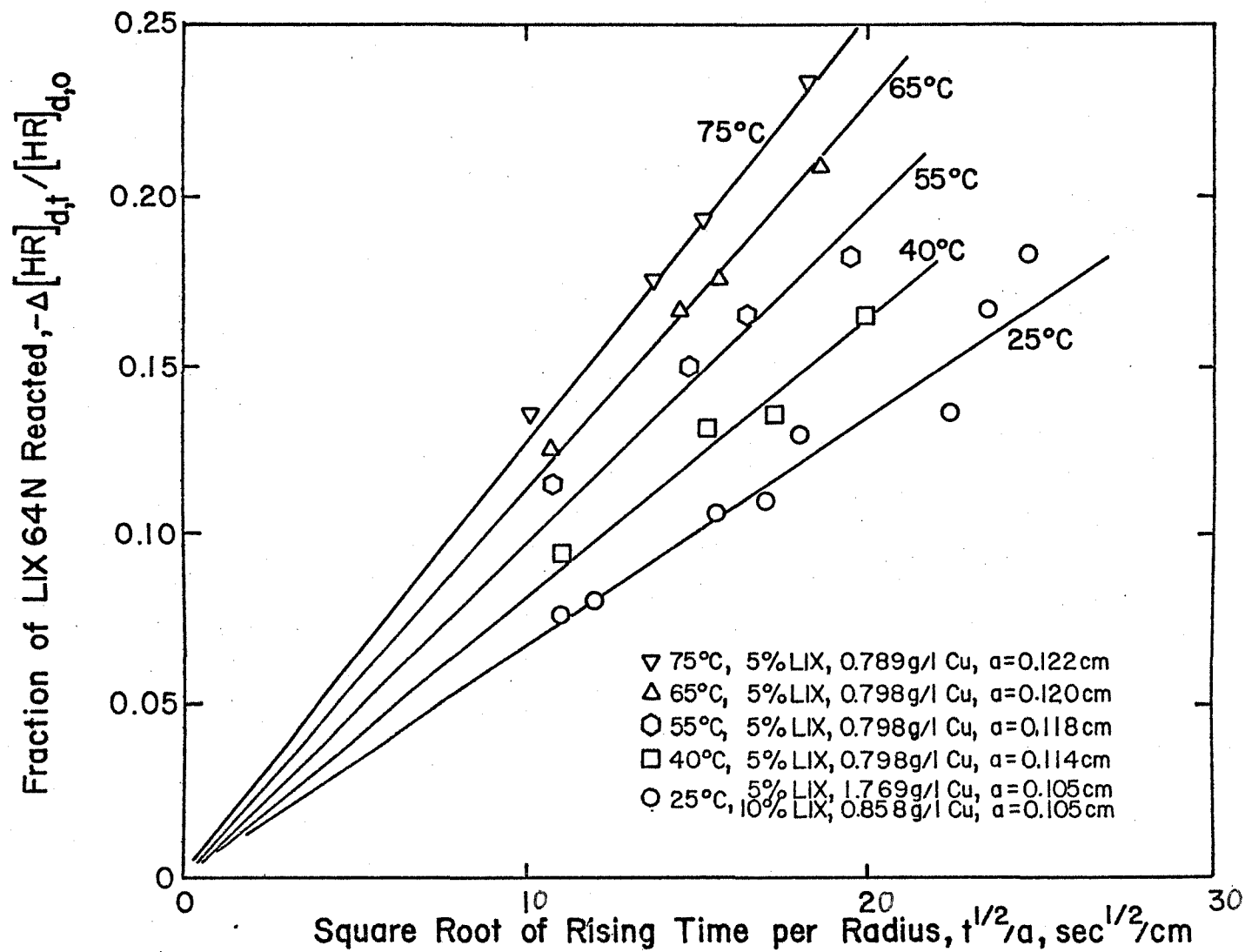


Figure 14. Parabolic plot of rate data for extraction into rising drops at various temperatures.

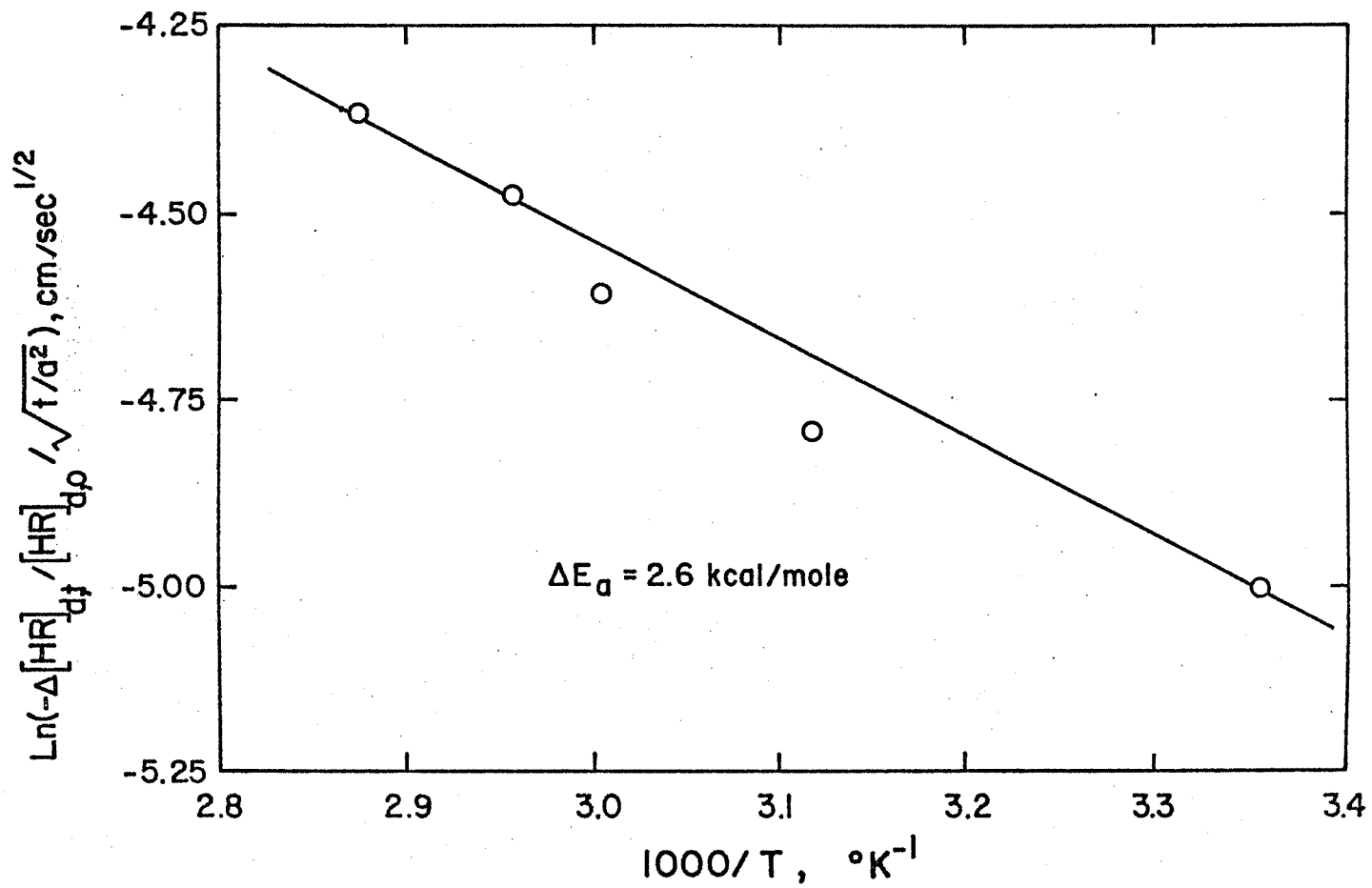


Figure 15. Arrhenius plot of the rate data presented in Figure 14.

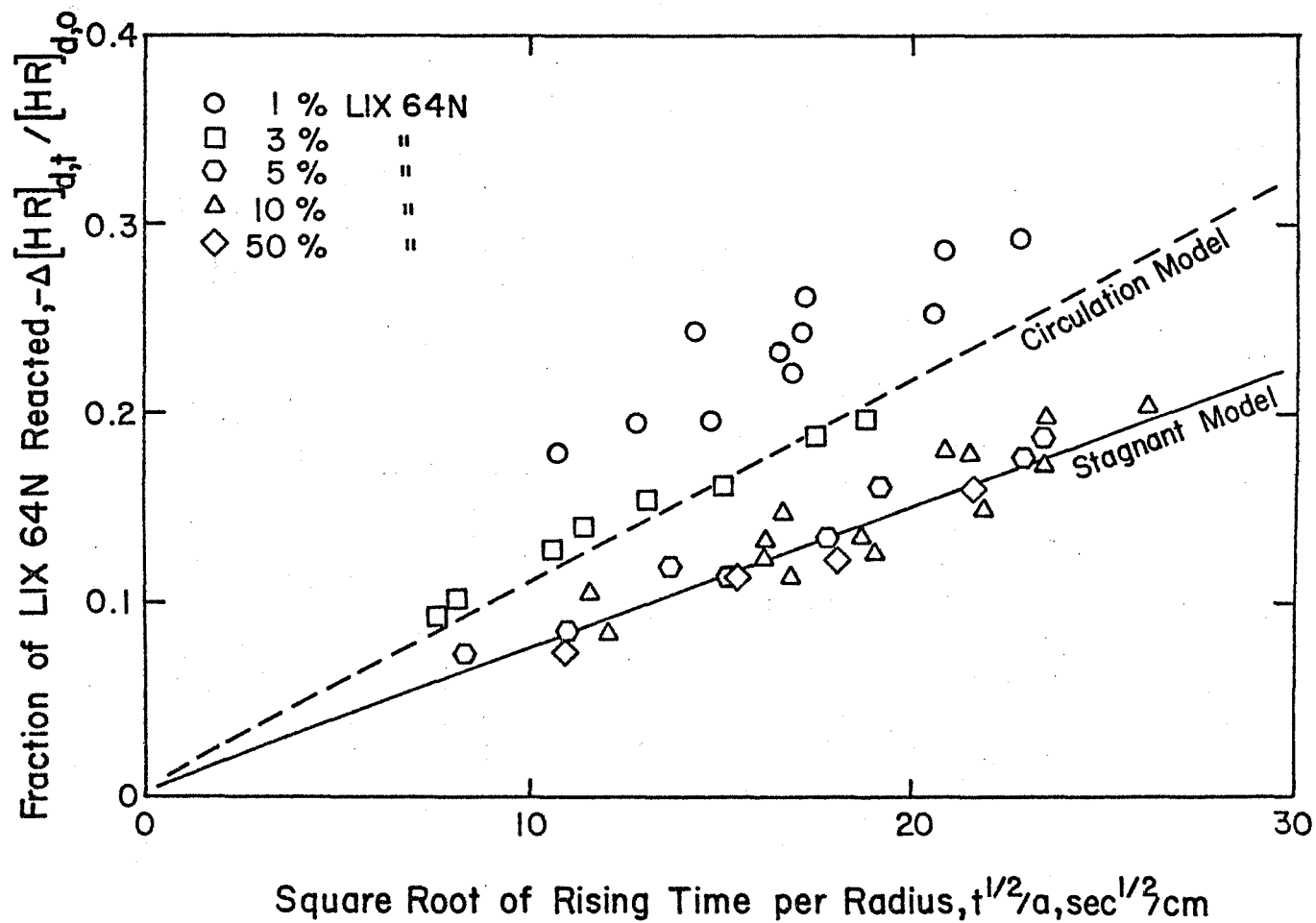


Figure 16. Comparison of experimental results with theoretical predictions for rate control by internal mass transfer (See equations 15 and 18) showing the concentration effect.

at low LIX concentrations. Figure 17 shows the effect of the drop size on the kinetics of the extraction. For small drop ($a = 0.108$ cm), the experimental data seems to be in the stagnant region; and for large drop ($a = 0.135$ cm) the experimental data seems to be close to the circulation region. These results are consistent with the expected hydrodynamic behavior of large drops which tend to circulate internally.

Kinetics of extraction with different LIX reagents. The kinetics of copper extraction by LIX 65N from acidic solution is slow and consequently LIX 63 is added to catalyze the reaction; the reaction kinetics being enhanced significantly. The mixture of LIX 65N and 1% LIX 63 is referred to as LIX 64N. In the ammoniacal system however, the rate appears to be limited by the transport of the reactant in the dispersed phase and under these circumstances should not be expected to be dependent on the composition and chemical properties of the extractant. Such is the case for the rate of copper extraction by LIX 64N, LIX 65N and LIX 54 as shown in Figure 18. All results follow the internal mass transfer model and the rates are insensitive to the chemical nature of the extractant. These results provide one more piece of evidence which supports rate control by transport in the dispersed phase. Note that no catalytic effect from LIX 63 is observed in the ammoniacal system.

Change in rate control from internal mass transfer to external mass transfer. As mentioned in the Introduction internal mass transfer is normally slower than external mass transfer. But the latter phenomenon can become the major rate limiting step if the initial concentration ratio $[Cu]_{c,0}/[HR]_{d,0}$ is less than 0.05. See Figure 3. Two experiments were

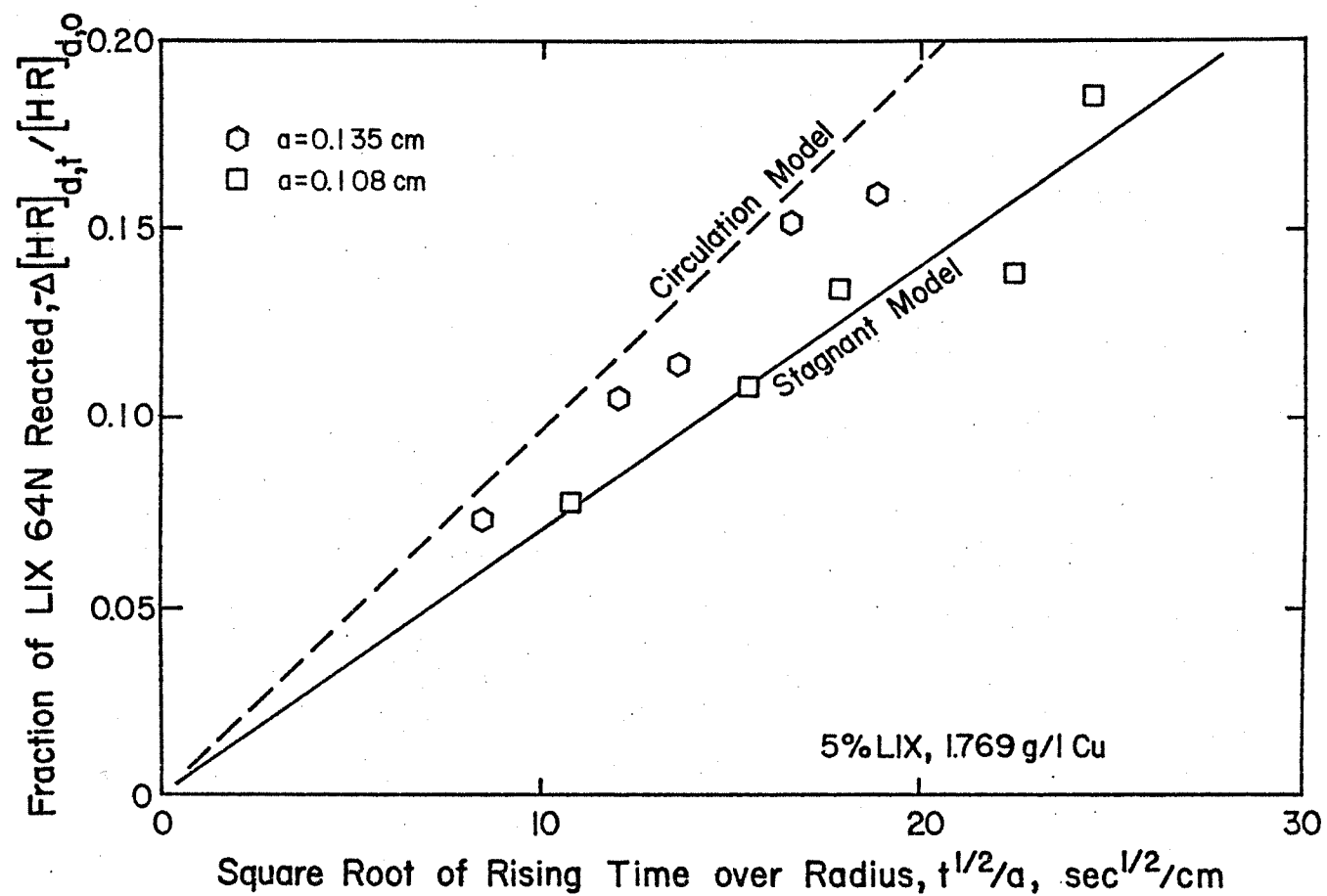


Figure 17. Comparison of experimental results with theoretical mass transfer showing the drop size effect.

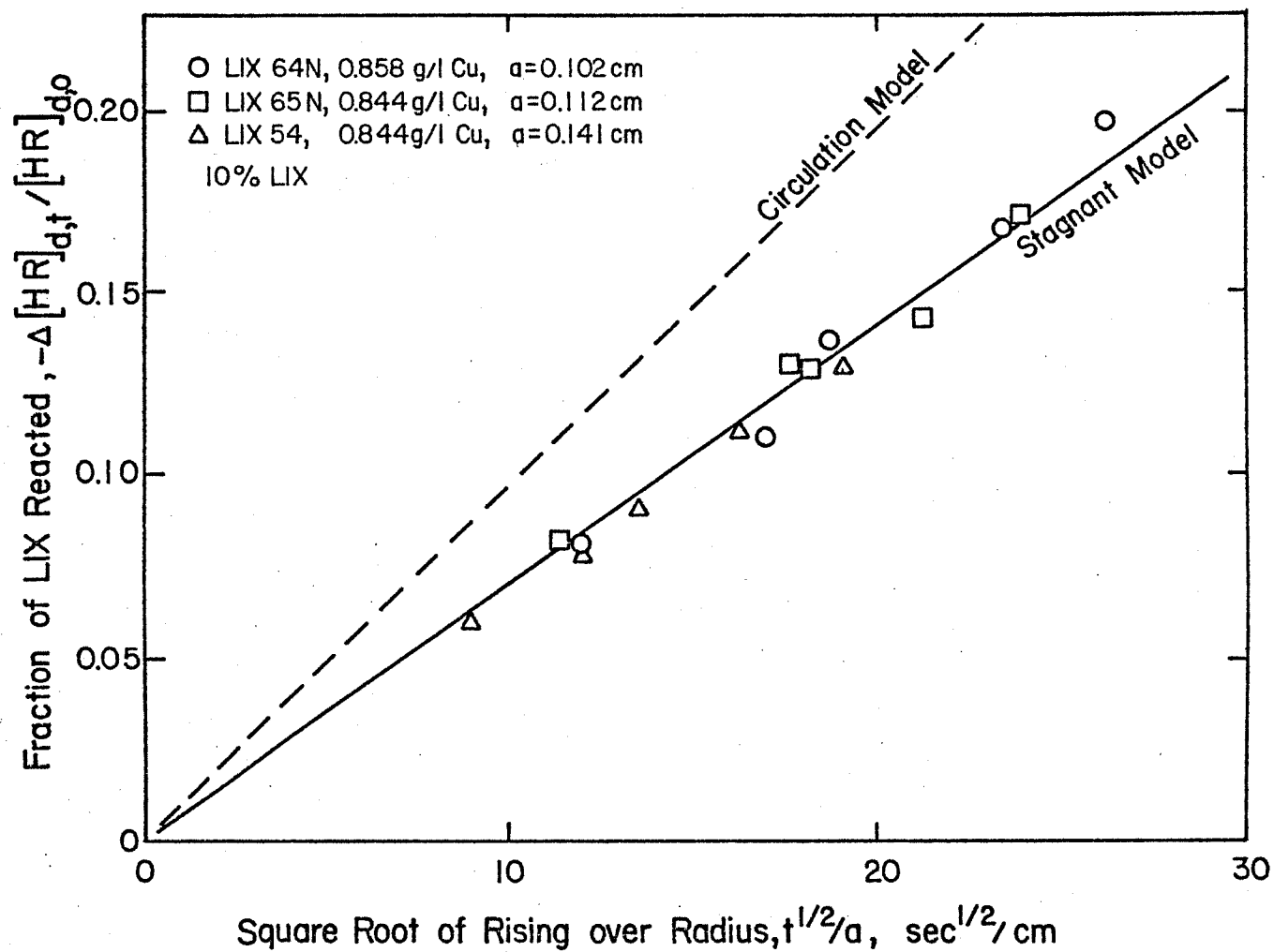


Figure 18. Parabolic plot of rate data for different chelating extractants. Note that the kinetics are essentially independent of the extractant and that 'no' catalytic effect from LIX 63 is observed.

done to test this hypothesis by selecting concentration ratios of 0.14 and 0.027. When the concentration ratio was 0.14, the experimental results, as expected, followed the stagnant model of internal mass transfer as shown in Figure 19. But when the concentration ratio was lowered to 0.027, the rate data fit the Levich model for external mass transfer as shown in Figure 20.

Falling Drop Experiments

In this series of experiments the aqueous phase and the organic phase were reversed. The aqueous phase became the dispersed drops and the organic solution became the continuous phase. Under these circumstances, of course, the drop fell through the continuous organic phase.

Effect of reactant concentration. If the reaction were still controlled by internal mass transfer, the rate would be dependent on the dispersed phase (aqueous) reactant (copper) concentration and independent of the continuous phase (organic) reactant (LIX 64N) concentration. [Recall that the rising drop experiments under most circumstances the rate had a first order dependence on the LIX concentration and was independent of the copper concentration because the LIX was the dispersed phase reactant and copper was continuous phase reactant.] The falling drop results, shown in Figures 21 and 22, indicate the rate increases as the copper concentration increases (Figure 21) and the rate does not change as the LIX 64N concentration increases. Again, as for the rising drops, the rate follows parabolic kinetics for both the small drop ($a = 0.087$ cm) shown in Figure 23, and the large drop ($a = 0.128$ cm) shown in Figure 24. Analysis of the rate constants shows that the kinetics

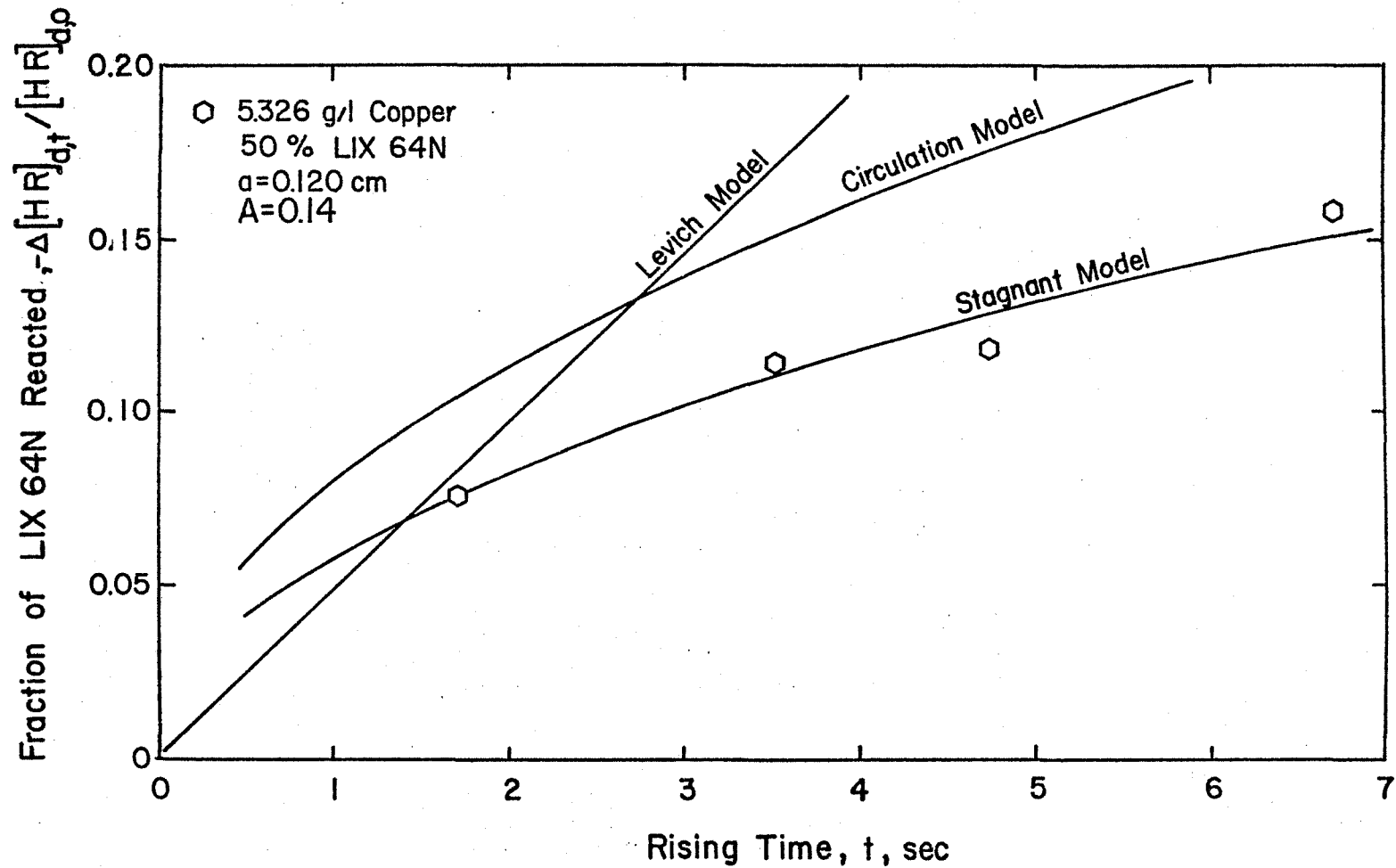


Figure 19. Evaluation of the "A" parameter, $(Cu)_{c,0} / (LIX)_{d,0}$ which theoretically determines the point at which external mass transfer resistance becomes predominant. For $A > 0.05$ reaction rates will be limited by internal mass transfer.

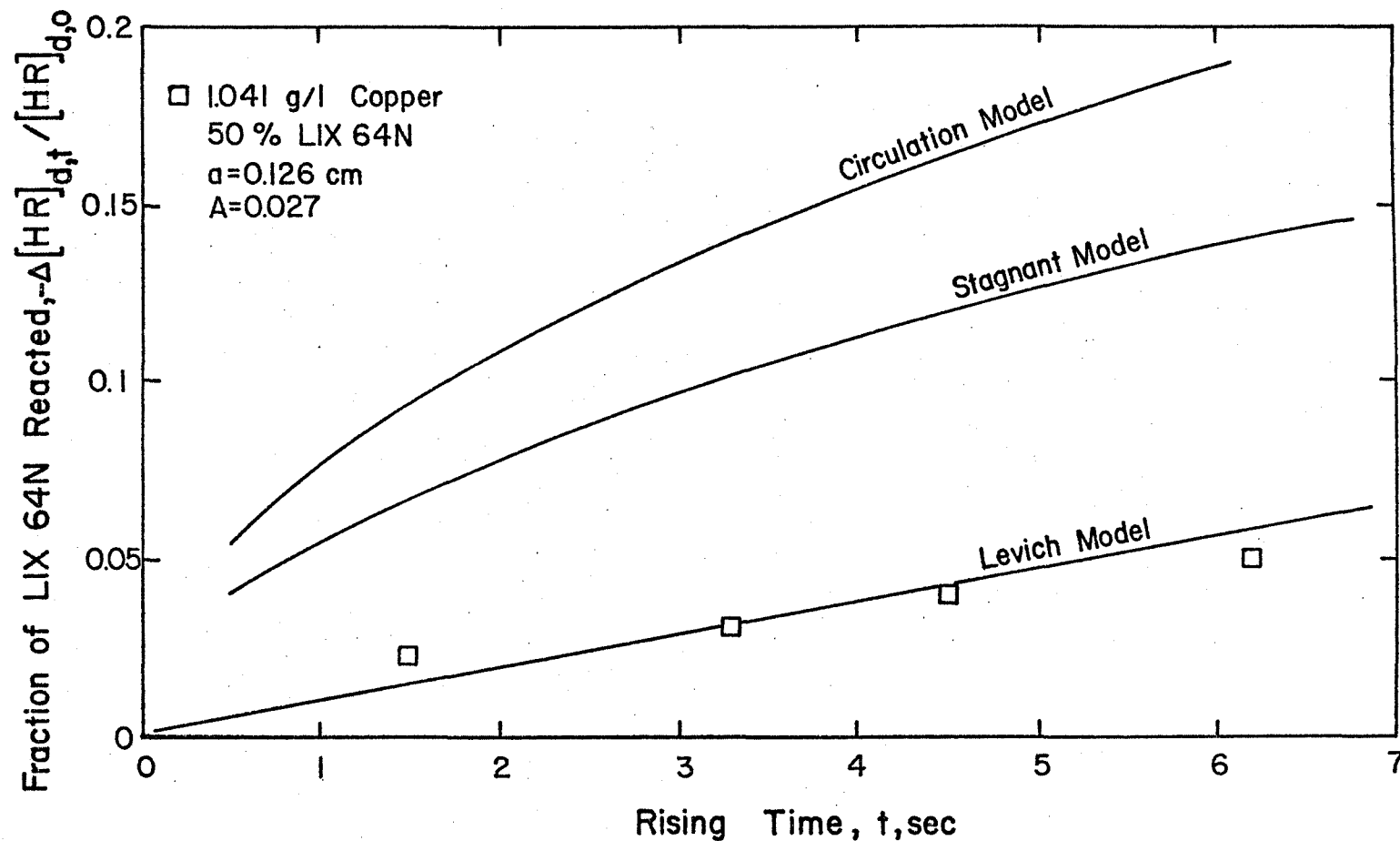


Figure 20. Evaluation of the parameter "A," $(Cu)_{c,0} / (LIX)_{d,0}$ which theoretically determines the point at which external mass transfer resistance becomes predominant. For $A < 0.05$ reaction rates will be limited by external mass transfer.

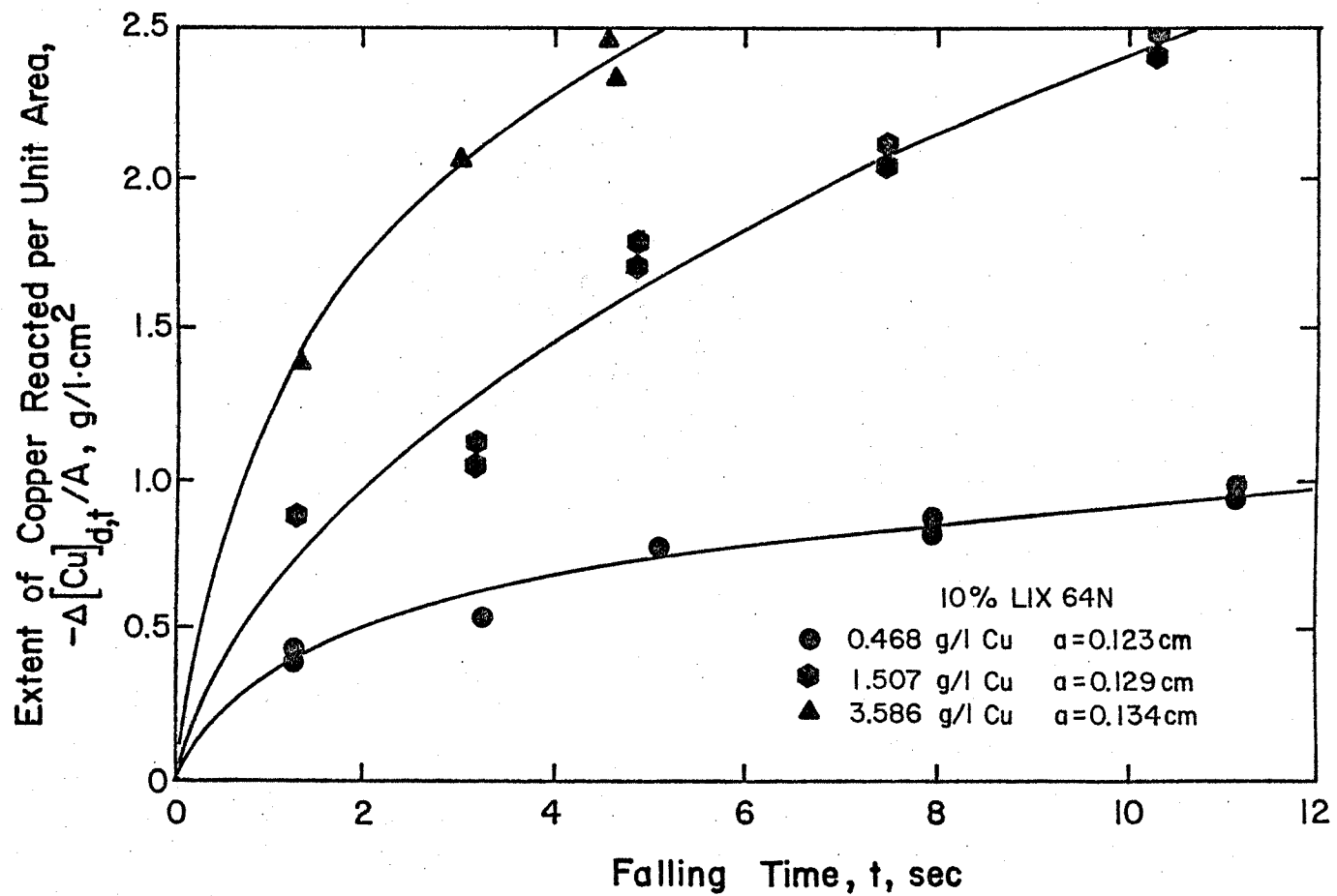


Figure 21. Rate of copper extraction from falling drops for various initial copper concentrations.

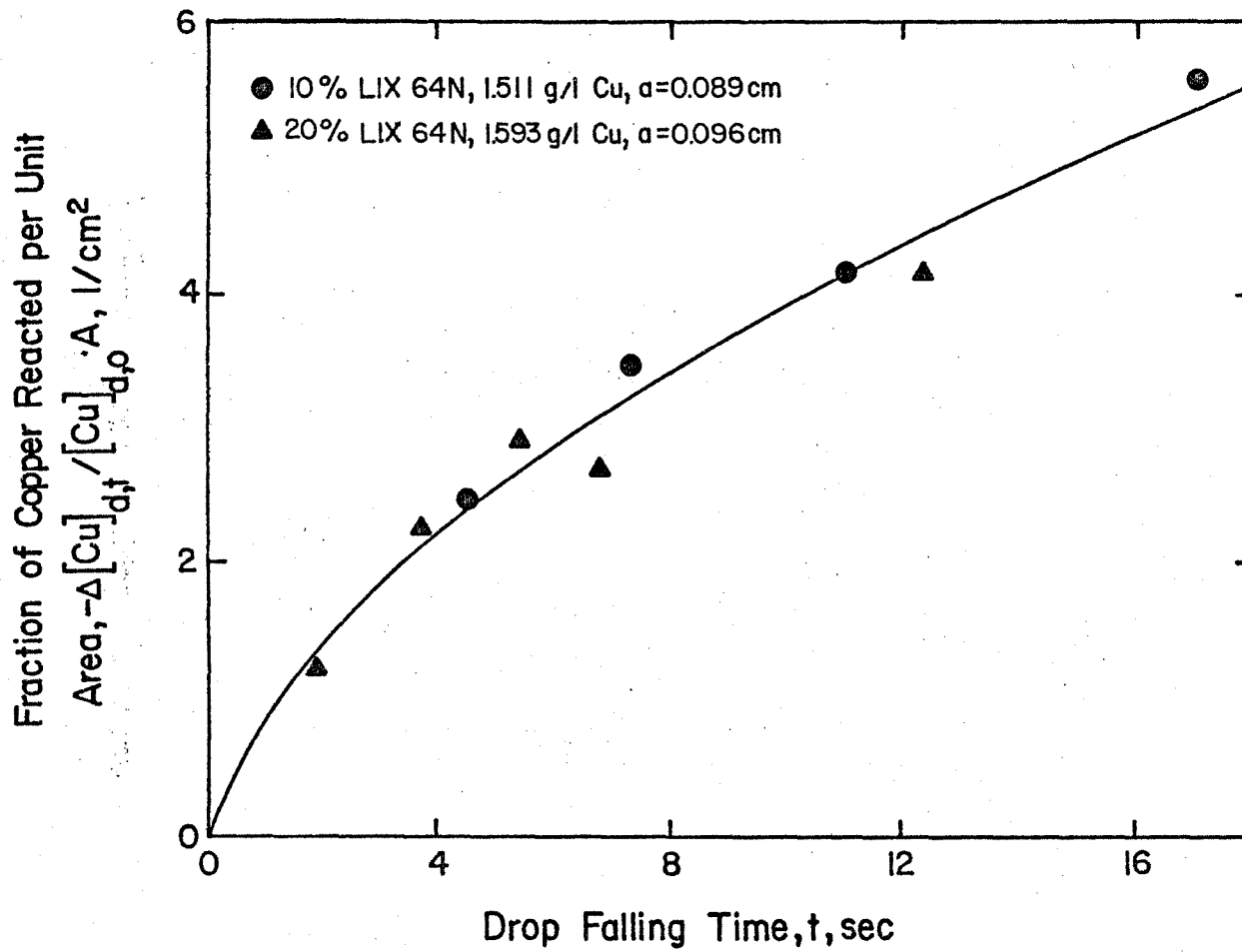


Figure 22. Rate of copper extraction from falling drops for various initial LIX 64N concentration.

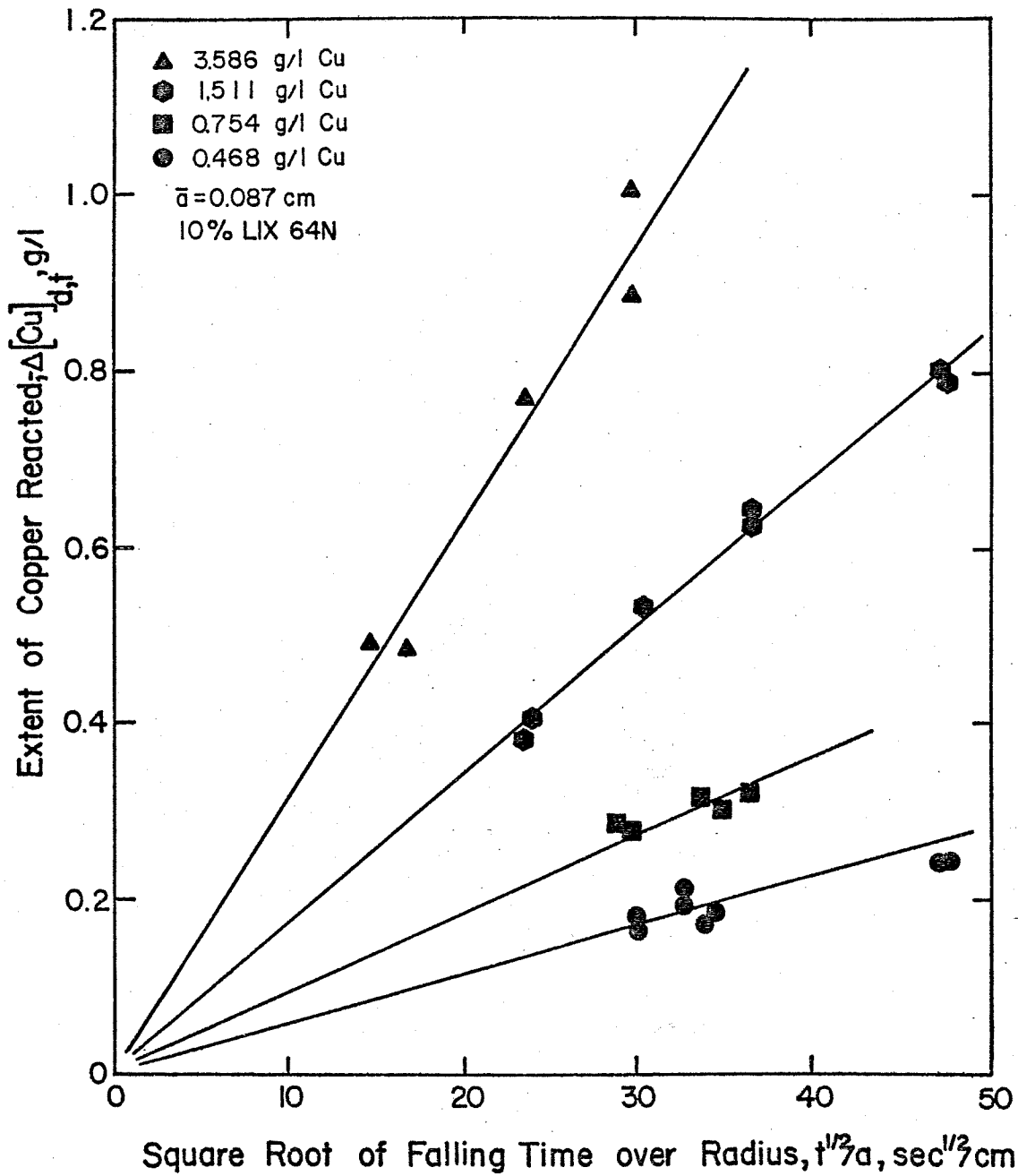


Figure 23. Parabolic plot of rate data for small drop size illustrating that the kinetics conform to the linear relationship required for rate control by internal mass transfer.

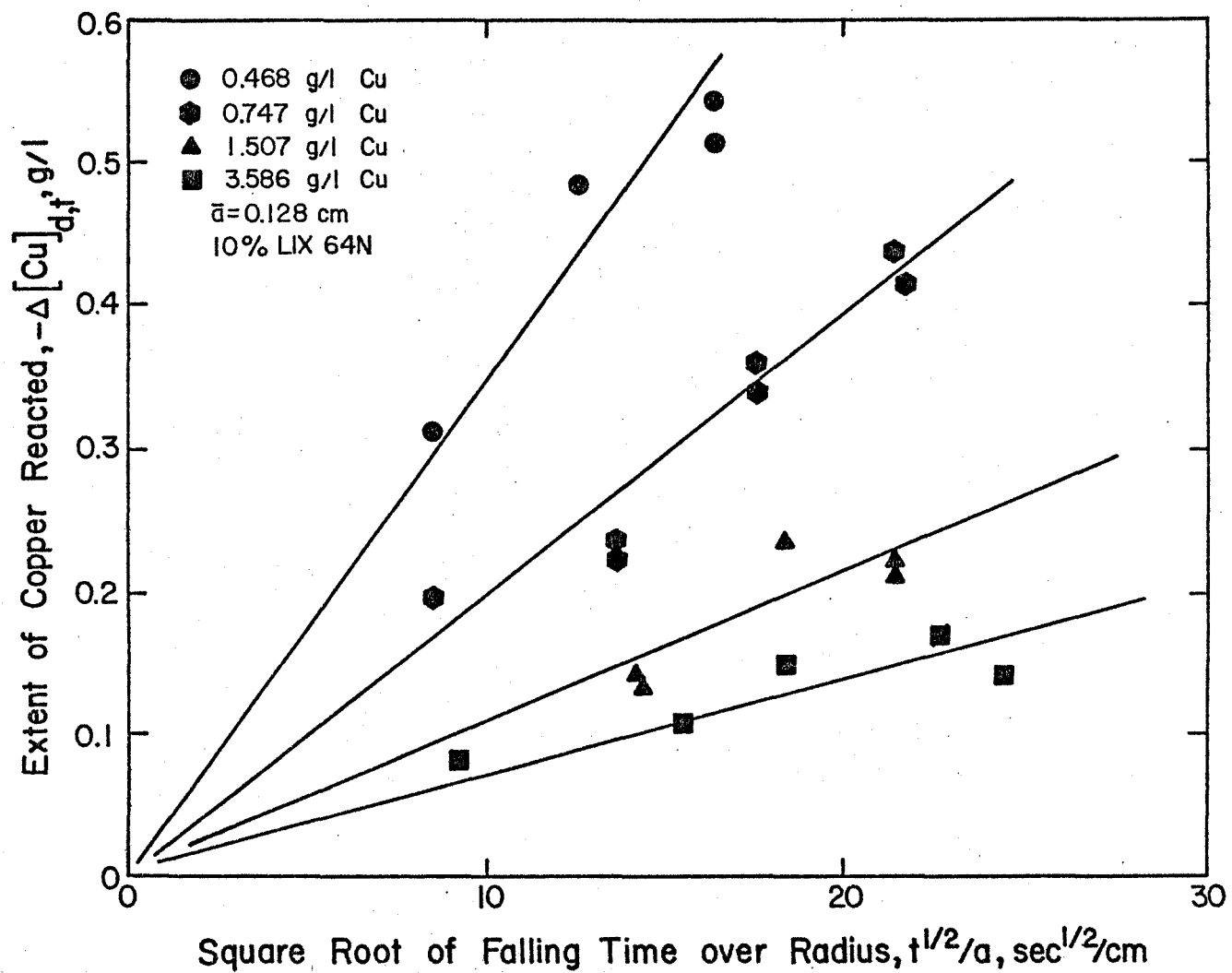


Figure 24. Parabolic plot of rate data for large falling drops illustrating that the kinetics conform to the linear relationship required for rate control by internal mass transfer.

are first order with respect to the copper concentration (See Figure 25) and suggests that the rate is still limited by internal mass transfer even when the phases are inverted.

Comparison of theory with experimental results. The mass transfer equations for the stagnant model and the circulation model can still be applied for the falling drop. However, the diffusing species is no longer the hydroxyoxime molecule but the copper-ammonia complex. The diffusion coefficient for the hydrated cupric ion has been reported in the literature to be $7.5 \times 10^{-6} \text{ cm}^2/\text{sec}$.⁽³⁰⁾ If the diffusion coefficient of copper ammonia complex is assumed to be the same as the hydrated cupric ion, the reaction rate can be predicted from first principles. Using equation 15 and 18 the comparison of experimental data with theoretical predictions is shown in Figures 26 and 27 where close agreement between theory and experiment is observed.

Figure 26 shows that as the copper concentration decreases the drops tend to circulate more. A similar effect was seen for rising drops when the hydroxyoxime concentration was reduced. However, for the same experimental conditions, the falling aqueous drops tend to circulate more than the rising drops. Compare Figures 26 and 16. This may be due to the viscosity effect i.e. more circulation for low viscosity drops. The viscosity of the aqueous drop for these conditions is about 1.0 cp while the viscosity of the organic drop is about 1.7 cp.

Figure 27 shows the effect of the drop size on kinetics of the extraction. Again the result reflect the anticipated hydrodynamic behavior in which large drops exhibit internal circulation.

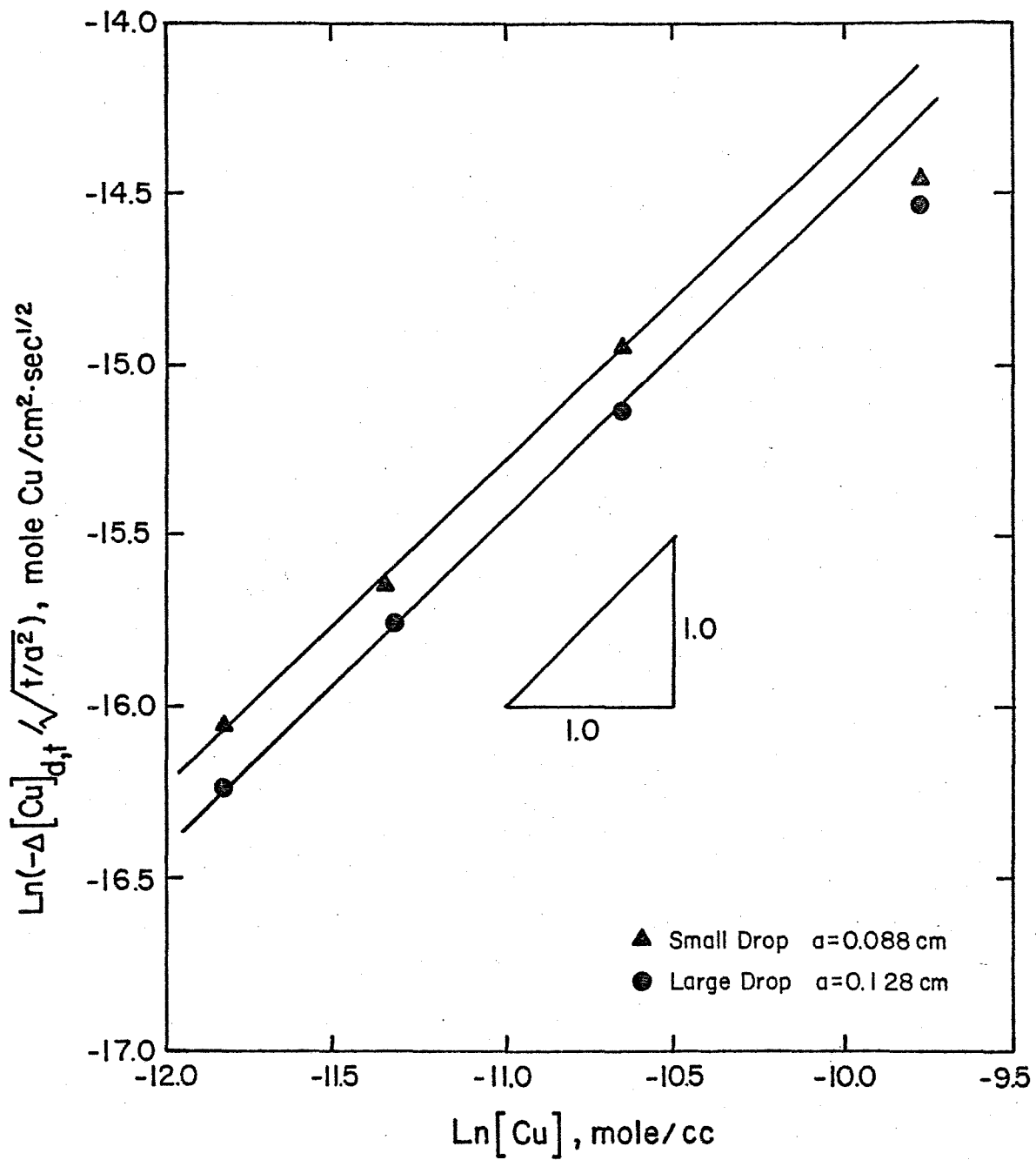


Figure 25. Reaction order plot illustrating the first order dependence on the copper concentration in the dispersed phase.

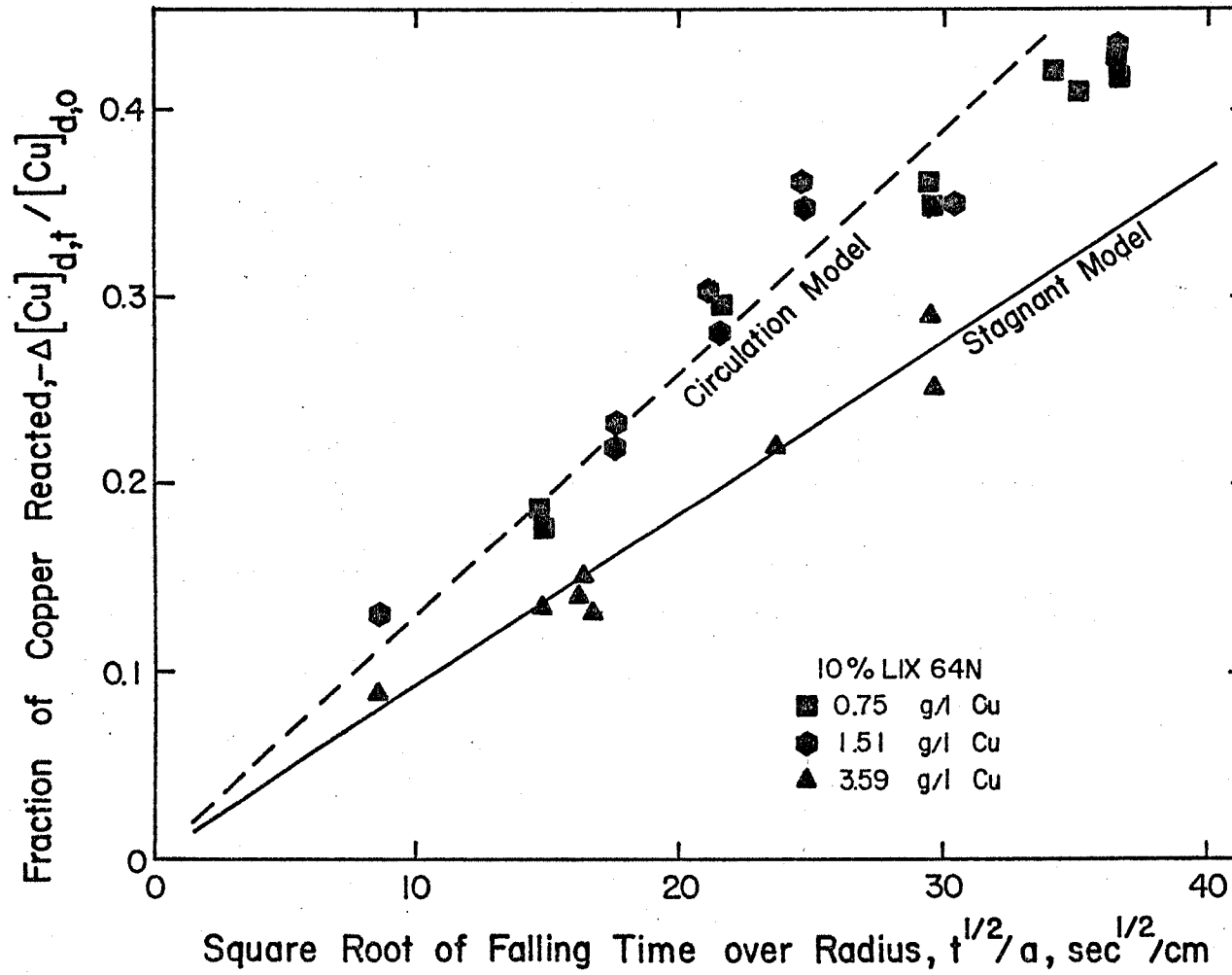


Figure 26. Comparison of experimental results with theoretical predictions for rate controlled by internal mass transfer for various copper concentrations (Eqs. 15 and 18). Data taken from Figures 22 and 23.

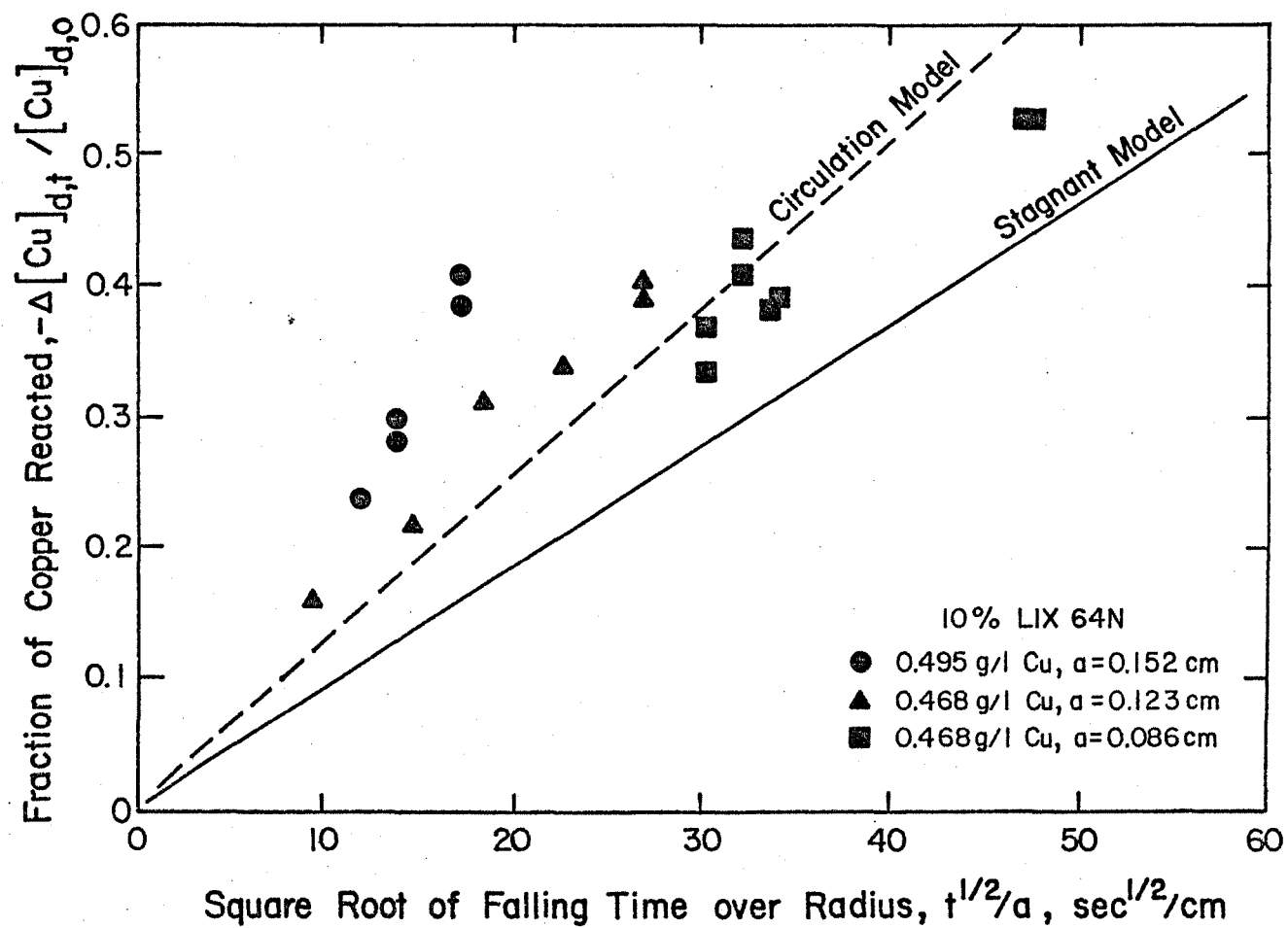


Figure 27. Comparison of experimental results with theoretical prediction for rate controlled by internal mass transfer for various drop sizes.

Figure 28 shows the combined effect of both concentration and drop size on the kinetics of extraction. As the concentration decreases or the drop size increases the amount of circulation increases.

All the experimental results provide strong evidence that extraction of copper by LIX 64N from ammoniacal solution is controlled generally by transport of the reactant in the dispersed phase. This result is quite different from the kinetics of copper extraction from acidic solution which has been shown to be a surface chemical reaction--controlled process. Figure 28 shows the difference in the reaction rates between extraction from ammoniacal solution and from acidic solution for similar experimental conditions. The rate of copper extraction from ammoniacal solution is about one order of magnitude greater than extraction from acidic solution. This observation reveals that the rate for these two cases is controlled by two different steps. Because the rate in the acid system is much slower than the slowest type of mass transport (stagnant model), and in view of other evidence, the rate is undoubtedly limited by the surface chemical reaction.^(6,7) The reason for the slow surface chemical reaction in acidic media may be due to the high polarity of coordinated water molecules in the primary coordination sheath of the cupric ion. At the aqueous/organic interface, the hydrated cupric ions prefer to orient themselves toward the aqueous phase via hydrogen bond linkage which results in a slow extraction process controlled by a chemical reaction step.

Drop Size Distribution in a Mixer

Development of an experimental technique to measure drop size distributions has been slow. Many difficulties have been encountered.

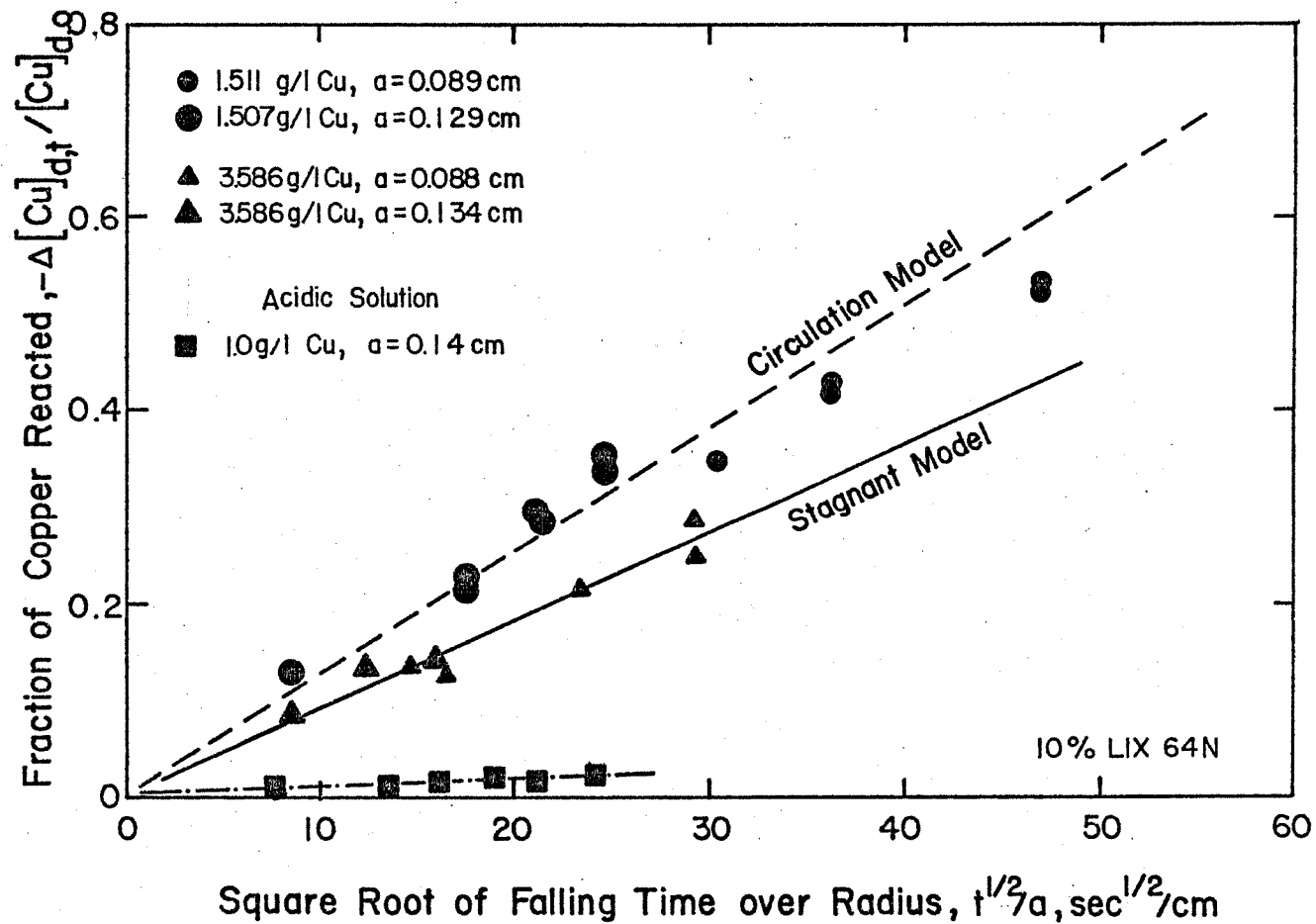


Figure 28. Combination effect of drop size and concentration on extraction kinetics compared with theoretical prediction for internal mass transfer. The kinetics of extraction in acidic solution is also shown which illustrate the rate is slower and not controlled by mass transfer process.

At this point it can be said that a population balance analysis of the breakage and coalescence events suggest that the steady state drop size distribution can, under certain idealized conditions, be described by the following exponential relationship,

$$f_0(v) = \frac{1}{v_0} \exp\left(-\frac{v}{v_0}\right) \quad (28)$$

where $f_0(v)$ = number drop size distribution density function in the mixer at steady state (cm^{-3}).

$f_0(v)dv$ = fraction of the total number of drops in the mixer whose size (volume) is in the range v to $v + dv$.

v_0 = number mean drop size, cm^3 .

As illustrated in Figure 29, this representation does provide a satisfactory description of previously published results.

Under certain circumstances, it may not be necessary to know details regarding the steady state drop size distribution in order to explain the rate of extraction which occurs in a mixer. For example, in the case of surface chemical reaction control, it is sufficient to know only the interfacial area. In this regard, correlation of interfacial area with specific power input for batch mixers has been reported.⁽³¹⁾ The interfacial area data can be represented by the following equation;

$$\bar{A} = 90 \bar{P}^{0.33} \quad (29)$$

where \bar{A} = interfacial area, cm^2/cm^3

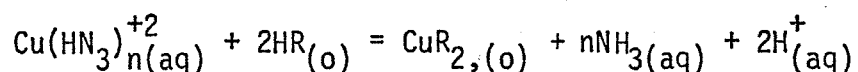
\bar{P} = specific power input, hp/1000 gal

CONCLUSIONS

The equilibrium state, the kinetics and the drop size distribution involved in copper extraction from ammoniacal solutions by hydroxyoxime extractants have been studied. The equilibrium study was done by shake-out tests, the kinetic experiments were carried out in a single drop reaction cell, and measurement of the drop size distribution in a mixer was accomplished by droplet stabilization followed by size analysis.

From the experimental results and the data analysis the following conclusions can be made.

1. Copper extraction from ammoniacal solution by hydroxyoxime extractants involves a complete displacement of ammonia ligands from the coordination sphere of the cupric ion. The chemical reaction can be written as,



2. The distribution coefficient is sensitive to the ammonia concentration and the pH of the system, which can be explained in terms of the stability of the various cupric ammonia complexes.

$$\log E = \log K - \log \left(1 + \sum_{i=1}^6 \beta_i [\text{NH}_3]_{(\text{aq})}^i \right) + 2 \log [\text{HR}]_{(\text{o})} + 2\text{pH}$$

3. From single drop experiments the kinetics of extraction appear to be controlled by mass transfer in the dispersed phase (irrespective of which phase is dispersed). The reaction has a low apparent activation energy of 2.6 kcal/mole.

4. The mass transfer process is explained to be due to molecular diffusion for small drop sizes, while convective transport contributes to the reaction rate for larger drop sizes.

5. The rate of copper extraction from ammoniacal solutions is faster than from acidic solutions. The latter is controlled by chemical reaction at the liquid/liquid interface. The reason for the slower kinetics in the acidic solution may be due to the higher polarity of water molecules that are coordinated to the cupric ion, causing an incompatibility with the nonpolar organic phase.

6. Droplet stabilization followed by size analysis was used to measure the drop size distributions generated in a stirred tank reactor with aqueous phase continuous. Results to date have not been conclusive, but a population balance analysis of breakage and coalescence events suggests that the steady state drop size distribution can be described by an exponential relationship.

REFERENCES

1. M.B. Shirts, P.A. Bloom and W.A. McKinney, "Double Roast-Leach Electro-winning Process for Chalcopyrite Concentrates," USBM R.I. 7006 (1975).
2. "In Clean-Air Production Arbiter Process is First Off the Mark," *Em/J*, 174, No. 2, 74 (1973).
3. R.D. Groves, T.H. Jeffers, and G.M. Potter, "Leaching Coarse Native Copper Ore with Dilute Ammonium Carbonate Solution," *Solution Mining Symposium, AIME*, 381 (1975).
4. R.L. Atwood and J.D. Miller, "Structure and Composition of Commercial Copper Chelate Extractants," *SEM/AIME, Trans.*, 254, 319 (1973).
5. J. Parrish, "Selective Liquid Ion Exchangers, II, Derivatives of Salicylaldehyde," *J. So. African Chem. Inst.*, 23, 129 (1970).
6. D.R. Spink and D.N. Okuhara, "Comparative Equilibrium and Kinetics of KELEX 100/120 and LIX 63/65N/64N Systems for Extraction of Copper," *International Symposium on Hydrometallurgy, AIME*, 497 (1973).
7. R.L. Atwood, D.N. Thatcher and J.D. Miller, "Kinetics of Copper Extraction from Nitrate Solutions by LIX 64N," *TMS/AIME Trans.*, 6B, 465 (1975).
8. D.S. Flett, D.N. Okuhara and D.R. Spink, "Solvent Extraction of Copper by Hydroxy Oximes," *J. Inorg. Nucl. Chem.*, Vol. 35, 2471 (1973).
9. C.A. Fleming, "The Kinetics and Mechanism of Solvent Extraction of Copper by LIX 64N and KELEX 100," *N.I.M. Report Johannesburg, S. Africa*, No. 1793, (1976).
10. S. Hu, and R.C. Kintner, "The Fall of Single Liquid Drops Through Water," *AIChE*, 1, No. 1, 42 (1955).
11. R.C. Kintner, "Drop Phenomena Affecting Liquid Extraction," *Advances in Chemical Engineering*, Drew ed., Academic Press, 4, 51 (1963).
12. A.I. Johnson and L. Braida, "The Velocity of Fall of Circulating and Oscillating Liquid Drops Through Quiescent Liquid Phase," *Can. J. Chem. Engr.*, Dec., 165 (1957).
13. H. Lamb, "Hydrodynamics," sixth ed., Cambridge Univ. Press, 450 (1932).
14. W.N. Bond, and D.A. Newton, "Bubbles, Drops and Stokes' Law," *Phil. Mag.* 6, (5), 794 (1927).

15. J. Crank, The Mathematics of Diffusion, Clarendon Press, Oxford, 2ed., 89 (1975).
16. R. Kronig and E.R. Brink, "On the Theory of Extraction from Falling Droplets," Appl. Sci. Res. A2, 143 (1950).
17. D.M. Rose and R.C. Kintner, "Mass Transfer from Large Oscillating Drop," AIChE. J., 12, 530 (1966).
18. V.G. Levich, Physicochemical Hydrodynamics, English Translation, Prentice-Hall, 395 (1962).
19. A.H.P. Skelland and A.R.H. Cornish, "Mass Transfer from Spheroids to an Air Stream," AIChE. J., 9, 73 (1963).
20. F.H. Garner and M. Tayeban, "The Importance of the Wake in Mass Transfer from both Continuous and Dispersed Phase System I., " Anales Real Sco. Espan. Fis. Quim. Sev. B-Quim, 56B, 479 (1960).
21. V.W. Uhl and J.B. Bray, Mixing, Vol. 1, Academic Press, New York (1966).
22. S. Nagata, Mixing Principles and Applications, John Wiley and Sons, New York (1975).
23. R. Mackelprang, "Variables Affecting Droplet Size Distribution in Liquid--Liquid Mixing Systems," Technical Notes in Metallurgy, University of Utah, Vol. 2, No. 3, (1978).
24. N.M. Rice, M. Nedved and G.M. Ritcey, "The Extraction of Nickel from Ammoniacal Media and its Separation from Copper, Cobalt and Zinc Using Hydroxyoxime Extractants," Hydrometallurgy, Vol. 3, No. 1, 35 (1978).
25. R.J. Whewell, M.A. Hughes and C. Hanson, "The Kinetics of the Solvent Extraction of Copper (II) with LIX Reagent," J. Inorg. Nucl. Chem., 37, 2303 (1975).
26. K. Durrani, C. Hanson, and M.A. Hughes, "Droplet Phenomena in the Ni/Na/D2EHPA/H₂O System," Met. Trans. B, AIME, 8B, 169 (1977).
27. C.R. Wilke and P. Chang, "Correlation of Diffusion Coefficients in Dilute Solutions," AIChE. J., 1, No. 2, 264 (1955).
28. M.A. Hughes, J.S. Preston and R.J. Whewell, "The Kinetics of the Solvent Extraction of Copper (II) with LIX 64N Reagent--II Activation Energies," J. Inorg. Nucl. Chem., 38 2067 (1976).
29. D.S. Flett, "Chemical Kinetics and Mechanisms in Solvent Extraction of Copper Chelates," Accounts of Chemical Research, 10, 99 (1977).

30. K.A. Smith, G.W. Lower, and W.A. Hockings, "Kinetics of Leaching Metallic Copper in Aqueous Cupric Ammonium Carbonate Solutions," International Symposium on Hydrometallurgy, Edited by D.J.J. Evans and R.S. Shoemaker, AIME, 265 (1973).
31. R.W. Luhnig and H. Sawistowski, "Phase Inversion in Stirred Liquid-Liquid Systems," paper 136 in Solvent Extraction, Proceedings of the International Solvent Extraction Conference, p. 873, Soc. Chem. Ind., London, England (1971).
32. D.E. Brown, and K. Pitt, Chem. Eng. Sci., Vol. 27, p. 577 (1972).
33. C.A. Coulaloglou and L.. Tavlarides, "Description of Interaction Processes in Agitated Liquid-Liquid Dispersions," Chem. Eng. Sci., Vol. 32, p. 1289 (1977).
34. F.H. Verhoff, S.L. Ross, and R.L. Curl. "Breakage and Coalescence Processes in the Agitated Dispersion, Experimental System and Data Reduction," Ind. Eng. Chem. Fundamentals, Vol. 16, p. 371 (1977).